Mon. Not. R. Astron. Soc. **378,** 245–275 (2007) doi:10.1111/j.1365-2966.2007.11771.x

Compressible turbulence in galaxy clusters: physics and stochastic particle re-acceleration

G. Brunetti[1]★ and A. Lazarian[2]

[1]*INAF – Istituto di Radioastronomia, via Gobetti 101, I-40129 Bologna, Italy*
[2]*Department of Astronomy, University of Wisconsin at Madison, 5534 Sterling Hall, 475 North Charter Street, Madison, WI 53706, USA*

Accepted 2007 March 22. Received 2007 February 8; in original form 2006 October 2

ABSTRACT

We attempt to explain the non-thermal emission arising from galaxy clusters as a result of the re-acceleration of electrons by compressible turbulence induced by cluster mergers. On the basis of the available observational facts we put forward a simplified model of turbulence in clusters of galaxies focusing our attention on the compressible motions. In our model intracluster medium (ICM) is represented by a high-beta plasma in which turbulent motions are driven at large scales. The corresponding injection velocities are higher than the Alfvén velocity. As a result, the turbulence is approximately isotropic up to the scale at which the turbulent velocity gets comparable with the Alfvén velocity. These motions are most important for the energetic particle acceleration, but at the same time they are subjected to most of the plasma damping. Under the hypothesis that turbulence in the ICM is highly super-Alfvénic the magnetic field is passively advected and the field lines are bended on scales smaller than that of the classical, unmagnetized, ion–ion mean free path. This affects ion diffusion and the strength of the effective viscosity. Under these conditions the bulk of turbulence in hot (5–10 keV temperature) galaxy clusters is likely to be dissipated at collisionless scales via resonant coupling with thermal and fast particles. We use collisionless physics to derive the amplitude of the different components of the energy of the compressible modes, and review and extend the treatment of plasma damping in the ICM. We calculate the acceleration of both protons and electrons taking into account both transit time damping acceleration and non-resonant acceleration by large-scale compressions. We find that relativistic electrons can be re-accelerated in the ICM up to energies of several GeV provided that the rms velocity of the compressible turbulent-eddies is $(V_{\rm L}/c_{\rm s})^2 \approx 0.15$–$0.3$; $c_{\rm s}$ is the sound speed in the ICM. We find that under typical conditions ≈2–5 per cent of the energy flux of the cascading of compressible motions injected at large scales goes into the acceleration of fast particles and that this may explain the observed non-thermal emission from merging galaxy clusters.

Key words: acceleration of particles – radiation mechanisms: non-thermal – turbulence – galaxies: clusters: general – radio continuum: general – X-rays: general.

1 INTRODUCTION

In the last years observations of galaxy clusters have shown that non-thermal components are mixed together with the thermal component of the intracluster medium (ICM). A fraction of massive galaxy clusters hosts diffuse radio emission in the form of radio haloes, Mpc-sized diffuse synchrotron radio sources at the cluster centre, and radio relics, elongated diffuse synchrotron radio sources at the cluster periphery. This directly proves the presence of GeV relativistic electrons (and/or positrons) and of μG magnetic fields diffused on Mpc scales through the cluster volume (e.g. Feretti 2005, for a review). A related issue is the discovery of non-thermal emission in the hard X-ray band detected in a few galaxy clusters (e.g. Fusco-Femiano et al. 2004; Rephaeli, Gruber & Arieli 2006).

The most spectacular example of non-thermal emission from galaxy clusters is that of giant radio haloes. These are very extended (Mpc) synchrotron radio emissions, not connected with cluster radio sources, at the centre of clusters, with a steep spectrum and a typical synchrotron

★E-mail: brunetti@ira.inaf.it

luminosity in the range $\approx 10^{40}$–10^{42} erg s^{-1}. A remarkable point is that the emitting particles have a lifetime considerably shorter than that necessary to diffuse over the scales of these radio haloes, and this poses a theoretical problem on their origin (e.g. Jaffe 1977). In principle if the content of cosmic ray hadrons in the ICM is sufficiently large, fast electrons and positrons may be continuously injected in the ICM via hadronic collisions between cosmic rays and thermal protons (Dennison 1980; Blasi & Colafrancesco 1999), alternatively different forms of *in situ* stochastic acceleration and re-acceleration operating for a small fraction of the cluster life may provide a viable source for high-energy emitting particles (Schlickeiser, Sievers & Thiemann 1987; Brunetti et al. 2001; Petrosian 2001). Future gamma ray observations (GLAST, *Cerenkov* telescopes) will constrain the content of cosmic ray hadrons in galaxy clusters and provide an important tool to better understand the origin of the relativistic particles in the ICM (e.g. Reimer 2004; Blasi, Gabici & Brunetti 2007, for recent reviews).

It is believed by several authors that the re-acceleration scenario may provide a promising picture to explain the bulk of present-day radio data (e.g. reviews by Brunetti 2003; Petrosian 2003; Brunetti 2004; Blasi 2004; Hwang 2004; Feretti 2005). This model essentially relies on the hypothesis that a fraction of the kinetic energy associated with cluster–cluster mergers is channelled into turbulence and re-acceleration of relativistic particles in the ICM.

MHD turbulence is known to be an important agent for particle acceleration since Fermi (1949) first pointed this out. Second-order Fermi acceleration by MHD turbulence was appealed for acceleration of particles in many astrophysical environments, for example, solar wind, solar flares, ICM, gamma-ray bursts (see Schlickeiser & Miller 1998; Chandran 2003; Brunetti et al. 2004; Petrosian & Liu 2004; Becker, Le & Dermer 2006; Cho & Lazarian 2006; Petrosian, Yan & Lazarian 2006; Dogiel et al. 2007). Naturally, properties of compressible MHD turbulence (see Shebalin, Matthaeus & Montgomery 1983; Higdon 1984; Montgomery, Brown & Matthaeus 1987; Shebalin & Montgomery 1988; Zank & Matthaeus 1992; Cho & Lazarian 2003, and references therein) are essential for understanding the acceleration mechanisms.

Among the advances in understanding MHD turbulence, we would like to mention the Goldreich & Sridhar (1995, hereafter GS95) model of turbulence. GS95 dealt with incompressible MHD turbulence and showed that Alfvén and pseudo-Alfvén modes follow the scale-dependent anisotropy of $l_\parallel \sim l_\perp^{2/3}$, where $l_\parallel$ is the size of the eddy along the local mean magnetic field and $l_\perp$ that of the eddy perpendicular to it. Lithwick & Goldreich (2001) conjectured that this scaling of incompressible modes is also true for Alfvén modes and slow modes in the presence of compressibility. In Cho & Lazarian (2002, 2003, hereafter CL03) the rational for considering separately the evolution of slow, fast and Alfvén mode cascades was justified. The numerical simulations in CL03 and Kowal & Lazarian (2006) verified that Alfvén and slow mode velocity fluctuations are indeed consistent with the GS95 scaling, while fast modes exhibit isotropy in both gas-pressure (high $\beta_{\rm pl}$) and magnetic-pressure (low $\beta_{\rm pl}$) dominated plasmas. The former case is the most appropriate for clusters of galaxies that we deal in this paper.

A single most important change in the paradigm that has become obvious recently is that if the turbulent-energy injection happens at large scales, the cascading Alfvénic mode is presented at sufficiently small scales by very elongated eddies. Thus the interactions of these modes with cosmic rays differ considerably from that of the isotropic eddies that earlier researchers dealt with. Under these conditions nearly isotropic fast modes were identified as the dominant agent for scattering and resonance acceleration (Yan & Lazarian 2002). As a consequence of this, our understanding of energetic particle–turbulence interactions via gyroresonance and the transit time damping (TTD) (Chandran 2000; Yan & Lazarian 2002; Farmer & Goldreich 2004; Yan & Lazarian 2004; Cassano & Brunetti 2005) as well as the non-resonance acceleration of cosmic rays by large-scale compressible motions (see Ptuskin 1988; Chandran 2003; Cho & Lazarian 2006) has been altered. This calls for the corresponding advances in the treatment of cosmic ray acceleration in the environment of clusters of galaxies (see e.g. Brunetti 2006; Lazarian 2006a).

2 OUTLINE OF THE PAPER

In this paper we proceed in three main steps.

(I) As a first point we discuss the problem of turbulence in the ICM and work up a simplified but physical picture of the properties and relevant scales of turbulence in galaxy clusters. As we discuss below (see Section 3.1) the plasma in clusters of galaxies is expected to be both magnetized and turbulent. Its Reynolds numbers are expected to vary as the magnetic field grow (Section 3.2), but they are expected to be high enough to allow turbulence to be excited. Finally, turbulence in hot galaxy clusters is expected to be dissipated via collisionless dampings and this makes the particle acceleration process a natural consequence (Section 3.4). This part of the paper is mainly designed to provide a reference picture for observers and a viable astrophysical starting point for theoretical developments.

(II) As a second point we discuss the physics of compressible motions in the collisionless regime. This part of the paper is a necessary extension of previous seminal studies of collisionless turbulence and is aimed at the presentation of necessary general equations to use in the paper. In particular to characterize the plasma–cosmic rays interactions we characterize the compressible motions using dielectric tensor (Section 4.1), give the expression for the energy spectrum of the fast modes in Section 4.2 and describe the TTD-damping in intracluster plasma in Section 4.3; complex expressions and calculations are reported in Appendices A–C.

(III) Finally, we discuss the issue of stochastic particle acceleration in galaxy clusters by compressible turbulence. The resonant TTD-acceleration is discussed in Section 5.1, while the effect of non-resonant acceleration is discussed in Section 5.2. In Section 6 we discuss the results in the framework of the particle re-acceleration model in galaxy clusters: in Section 6.1 we briefly review the basic physics of cosmic rays in galaxy clusters, and in Section 6.2 we present detailed calculations on particle re-acceleration in the ICM. Here we claim that compressible turbulence may drive efficient particle acceleration in the ICM. This is an extension of recent studies on the argument and provides a view of the process of particle re-acceleration in the ICM which is additional (or alternative) to that of Alfvénic acceleration.

In Section 7 we discuss the most relevant findings and simplifications, and in Section 8 we provide a short summary.

3 TURBULENCE IN THE ICM

3.1 Injection of turbulence in the ICM

Cluster mergers and accretion of matter at the virial radius may induce large-scale motions with $V_{\rm L} \sim 1000\,{\rm km\,s^{-1}}$ in massive clusters. Numerical simulations suggest that turbulent motions may store an appreciable fraction, 5–30 per cent, of the thermal energy of the ICM (e.g. Sunyaev, Norman & Bryan 2003; Dolag et al. 2005; Vazza et al. 2006). Simulations of merging clusters provide an insight into the gas dynamics during a merger event (e.g. Roettiger, Burns & Loken 1996; Roettiger, Loken & Burns 1997; Ricker & Sarazin 2001): subclusters generate laminar bulk flows through the sweeped volume of the main clusters which inject turbulence via, for example, Kelvin–Helmholtz instabilities at the interface of the bulk flows and the primary cluster gas. The largest turbulent eddies decay into smaller and turbulent velocity fields developing a turbulent cascade.

A simple, but well motivated by physical arguments, semi-analytical approach allows to follow the cosmological injection of merger-turbulence. Calculations from Cassano & Brunetti (2005) suggest that turbulence in the ICM is transient being mostly injected during the most massive mergers. However, since more frequent minor mergers may also contribute to the injection of such turbulence, some minimum level of turbulence should be rather ubiquitous in the ICM. In these calculations turbulence is assumed to be injected in the cluster volume swept by the subclusters, which is bound by the effect of the ram-pressure stripping, and the turbulent energy is calculated as a fraction of the $P\,{\rm d}V$ work done by the subclusters falling in to the main cluster. Essentially merger-driven turbulence is powered by the gravitational potential well and thus the energy of this turbulence should approximately scale with the cluster thermal energy (Cassano & Brunetti 2005). Support to this scaling comes from a recent analysis of a sample of galaxy clusters from cosmological numerical simulations (Vazza et al. 2006).

Turbulence is an important ingredient in the physics of the ICM as it is necessary to understand the amplification of magnetic fields in clusters (Dolag, Bartelmann & Lesch 2002; Schekochihin et al. 2005; Subramanian, Shukurov & Haugen 2006), an issue closely related to the non-thermal emission from clusters but that we will not address in this paper. Turbulence might provide a source of heating to balance the cooling of cluster cores (Fujita, Matsumoto & Wada 2004), and the knowledge of the basic aspects of turbulence in galaxy clusters is also crucial to model the transport of heat and metals in the ICM (Narayan & Medvedev 2001; Cho et al. 2003; Voigt & Fabian 2004; Lazarian 2006b).

In spite of obvious observational challenges, indications of some level (at least 10–20 per cent of the thermal energy) of turbulence in the ICM comes from gas-pressure maps in the X-rays (Schuecker et al. 2004), and also from the lack of resonant scattering from X-ray spectra (Churazov et al. 2004; Gastaldello & Molendi 2004).

Interestingly enough, also upper limits to the turbulent-energy content in the ICM were obtained in a few nearby galaxy clusters from kinematical arguments related to the properties of Hα and X-ray filaments (e.g. Fabian et al. 2003; Crawford et al. 2005; Sun et al. 2006). Assuming that turbulence is driven at hundred-kpc scales the above upper limits actually can be used to place upper limits on the intensity of strong turbulence in the ICM (supersonic or trans-sonic turbulence).

3.2 Reynolds number and developing of turbulence in the ICM

In this section we discuss the important issue of the Reynolds number of the fluid in the ICM, and derive its value by assuming a simple, but physically motivated, scenario.

A fluid becomes turbulent when the rate of viscous dissipation at the injection scale, $L_{\rm o}$, is much smaller than the energy transfer rate, that is, when the Reynolds number is $Re = V_{\rm L}L_{\rm o}/\nu_{\rm K} \gg 1$, where $V_{\rm L}$ is the injection velocity and $\nu_{\rm K}$ is the kinetic fluid viscosity. The main source of uncertainty here comes from our ignorance of $\nu_{\rm K}$ in the ICM.

If the ICM were not magnetized $\nu_{\rm K} \sim l_{\rm mfp}v_{\rm i}/3$, were $v_{\rm i}$ is the velocity of thermal ions, and $l_{\rm mfp}$ is the ion–ion mean free path *in case of pure Coulomb interactions* (e.g. Braginskii 1965):

$$l_{\rm mfp} \sim 15\,000 \left(\frac{n_{\rm e}}{10^{-3}\,{\rm cm^{-3}}}\right)^{-1} \left(\frac{T}{8\,{\rm keV}}\right)^{2} \left(\frac{40}{\ln\Lambda}\right) \quad ({\rm pc}), \tag{1}$$

where $\ln\Lambda$ is the Coulomb logarithm.

Thus the corresponding Reynolds number would be

$$Re \sim 52 \left(\frac{V_{\rm L}}{1000\,{\rm km\,s^{-1}}}\right) \left(\frac{L_{\rm o}}{300\ {\rm kpc}}\right) \left(\frac{n_{\rm th}}{10^{-3}\,{\rm cm^{-3}}}\right) \left(\frac{T}{8\,{\rm keV}}\right)^{-5/2} \left(\frac{\ln\Lambda}{40}\right) \tag{2}$$

which is formally just sufficient for initiating the developing of turbulence.

However, in the presence of (even a small) *stationary* magnetic field the Reynolds number for motions in the direction perpendicular to the magnetic field gets extremely high essentially because the perpendicular mean free path of particles is limited to the Larmor gyroradius-scale (e.g. Braginskii 1965). Potentially, diffusion along the wandering turbulent-magnetic field lines could significantly increase the particle diffusivity and the plasma viscosity. For instance, estimates in Narayan & Medvedev (2001) suggest that electron diffusivity in a turbulent

medium can be of the order of 1/5 of the classical Spitzer value for unmagnetized medium, provided that the injection velocity, $V_{\rm L}$, is equal to the Alvén velocity.

More general calculations (Lazarian 2006a, and references therein) show that things could be more complicated and that the effective viscosity depends on the super- or sub-Alfvénic nature of the turbulence.[1] Turbulence in the ICM is super-Alfvénic, that is, turbulence with the injection velocity larger than the Alfvén one. In this case the turbulent hydrodynamic motions can easily bend the magnetic field lines. The trajectory of the particle that follows such a field line gets diffusive even in the absence of collisions. The effective mean free path of a particle is determined by the scale at which magnetic tension can withstand the hydrodynamic forces, that is, the scale at which the turbulent velocity, $V_{l_{\rm A}}$, gets equal to the Alfvén one, $v_{\rm A} = B/\sqrt{4\pi\rho}$, where $B \sim (B_{\rm o}^2 + B_{\rm rms}^2)^{1/2}$, (Lazarian 2006b). This scale, at which turbulence becomes MHD, is[2] $l_{\rm A} \sim L_{\rm o}(v_{\rm A}/V_{\rm L})^3$ and assuming typical conditions in Mpc regions at the centre of massive (and hot) galaxy clusters where radio haloes are found, it is

$$l_{\rm A} \sim 100 \left(\frac{B}{\mu{\rm G}}\right)^3 \left(\frac{L_{\rm o}}{300\ {\rm kpc}}\right) \left(\frac{V_{\rm L}}{10^3\ {\rm km\ s^{-1}}}\right)^{-3} \left(\frac{n_{\rm th}}{10^{-3}\ {\rm cm^{-3}}}\right)^{-3/2} \quad ({\rm pc}) \tag{3}$$

which is $< l_{\rm mfp}$. This implies the important point that, even for motions along the magnetic field, the Reynolds number in a turbulent ICM is larger than that estimated with the classical formula (equation 2). Actually one finds $Re >$ few times 10^3 which ensures that the ICM gets turbulent.

The main uncertainty in the evaluation of the Reynolds number comes from the value of the effective mean free path of particles. Equation (3) accounts for the effect of the turbulent magnetic field, however additional mechanisms may affect the value of the particle mean free path in the ICM, for example, plasma instabilities. Plasma instabilities could be at work in the ICM, for example, turbulent compressions themselves may drive instabilities. These instabilities in the ICM may induce scatterings of thermal ions *which reduce the effective mean free path and further increase the value of the Reynolds number* (e.g. Lazarian & Beresnyak 2006; Schekochihin & Cowley 2006). In what follows to be conservative and with the aim to simplify the overall picture, we disregard this effect, so that our estimates of the Reynolds number in the ICM would be considered as a lower limit.

3.3 Turbulent modes

3.3.1 Basic properties of the turbulent modes

Turbulence discussed in the previous sections is a complex mixture of several turbulent modes. The ICM is a compressible high-beta plasma. At large scales, where magnetic fields are not dynamically important ($V_{\rm L} \gg v_{\rm A}$), the turbulence is essentially in the hydro-regime, and we shall assume that turbulence in the ICM is done by solenoidal and compressible (essentially sound waves) motions. At smaller scales, in the MHD regime, it is $V_l \leqslant v_{\rm A}$ and three types of modes should exist in a compressible magnetized plasma: Alfvén, slow and fast modes. Slow and fast modes may be roughly thought as the MHD counterpart of the compressible modes, while Alfvén modes may be thought as the MHD counterpart of solenoidal Kolmogorov eddies (a more extended discussion can be found in Cho, Lazarian & Vishniac 2002, and references therein). Sound modes at large scales have propagation properties similar to that of the fast modes in the MHD regime. For this reason in this paper we shall use the properties of these modes for describing compressible turbulence, that is, hydro-modes (sound waves) at large scales and fast modes themselves at small scales. Fast modes are compressive waves which propagate across or at an angle to the local magnetic field. The fast-mode branch in a plasma extends from low frequencies up to the electron cyclotron frequency. At frequencies below the ion cyclotron frequency, and in the weak damping limit, the dispersion relation of these modes is given by $\omega = V_{\rm ph}k$, where the phase velocity is given by (e.g. Krall & Trivelpiece 1973)

$$V_{\rm ph}^2 = \frac{c_{\rm s}^2 + v_{\rm A}^2}{2} \left[1 + \sqrt{1 - 4\left(\frac{k_\parallel}{k}\right)^2 \frac{c_{\rm s}^2 v_{\rm A}^2}{\left(c_{\rm s}^2 + v_{\rm A}^2\right)^2}}\right] = \frac{c_{\rm s}^2}{\beta_{\rm pl}} \left(\frac{\beta_{\rm pl}}{2} + 1\right) \left[1 + \sqrt{1 - 4\left(\frac{k_\parallel}{k}\right)^2 \frac{\beta_{\rm pl}/2}{(1+\beta_{\rm pl}/2)^2}}\right] \stackrel{\beta_{\rm pl}\gg 1}{\longrightarrow} c_{\rm s}^2 \tag{4}$$

and where the parameter beta of the plasma is defined by $\beta_{\rm pl} = 2c_{\rm s}^2/v_{\rm A}^2$.

Alfvén modes propagate along or at an angle to the local magnetic field. The Alfvén branch extends from low frequencies up to the ion cyclotron frequency. In this frequency range the Alfvénic dispersion relation is given by $\omega = v_{\rm A}|k_\parallel|$, where $v_{\rm A} = B_{\rm o}/\sqrt{4\pi n_{\rm th} m_{\rm i}}$ is the Alfvén velocity.

Alfvén and fast modes differ also for the direction of the displacement vectors: the displacement of Alfvén modes is always perpendicular to $B_{\rm o}$, while that of fast modes makes an angle to the local magnetic field and in the case $\beta_{\rm pl} \to 0$ it is perpendicular to $B_{\rm o}$, while for $\beta_{\rm pl} \to \infty$ it becomes radial (along k); a detailed discussion on the decomposition of MHD modes can be found in Cho & Lazarian (2002, 2003) and in Kowal & Lazarian (2006).

Slow modes has '$-$' before the square root in equation (4) and for $\beta_{\rm pl} \gg 1$ they have the dispersion relation of Alfvén modes. We will not include slow modes in our calculations in the in the particle acceleration process by large-scale modes (Section 5) as they have a phase velocity in the ICM much smaller than that of the fast modes and thus are less important.

[1] The super- and sub-Alfvénic are determined in terms of the total magnetic field.
[2] In deriving equation (3) we use the hydro-scaling $V_l \propto l^{1/3}$.

At MHD scales Alfvén and slow modes might be of some relevance in discussing the particle acceleration process either because they can accelerate particles, or because in principle they may provide a particle pitch-angle scattering process[3] which is required by acceleration processes driven by other modes (Sections 4 and 5).

3.3.2 Coupling between turbulent modes in the ICM

Although the complex dynamics of galaxy clusters and the relatively large value of the Reynolds number of the ICM are likely to make the ICM itself a turbulent medium, it is somewhat difficult to have a clear idea of the relative importance of the different turbulent modes in the ICM. Indeed this depends on the nature of the turbulent forcing and on the mode coupling between different modes in the ICM.

We shall assume that a sizeable part of turbulence at large scales (viz. at scales where the magnetic tension does not affect the turbulent motions) is in the form of compressible motions. This is reasonable as these modes are expected to be easily generated in a high-beta medium even in the unfavourable case of solenoidal turbulent forcing. This is proved by closure calculations carried out in the case of $\beta_{\rm pl} \gg 1$. Indeed when motions are hydro in nature the coupling between solenoidal and compressible motions is efficient and the excitation of compressible modes by the solenoidal modes is driven by the *incompressible* pressure arising from non-linear interaction between solenoidal modes themselves (Bertoglio, Bataille & Marion 2001). These studies have shown that the fraction of energy in the form of compressible modes is found to scale with $\propto M_{\rm s}^2 \times Re$ for $M_{\rm s}^2 \times Re < 10$ ($M_{\rm s} < 1$ is the turbulent Mach number), while for $M_{\rm s}^2 \times Re \geqslant 10$ the scaling is expected to flatten (Zank & Matthaeus 1993; Bertoglio et al. 2001). Obviously a solenoidal turbulent forcing, which limits the energy of compressible modes to be smaller than that of solenoidal modes (even in the super-Alfvénic case), is probably not appropriate for galaxy clusters where turbulence is likely to be excited by compressible forcings, and this might result in a larger ratio between compressive and solenoidal modes (at least for super-Alfvénic motions).

Situation may be radically different at smaller scales where the magnetic field tension affects turbulent motions, that is, in the MHD regime, $l \leqslant l_{\rm A}$. In this case, MHD numerical simulations have shown that a solenoidal turbulent forcing gets the ratio between the amplitude of Alfvén and fast modes in the form CL03:

$$\frac{(\delta V)_c^2}{(\delta V)_{\rm s}^2} \sim \frac{(\delta V)_{\rm s} v_{\rm A}}{c_{\rm s}^2 + v_{\rm A}^2} \tag{5}$$

which essentially means that coupling between these two modes may be important only at $l \approx l_{\rm A}$ (in the MHD regime it should be $(\delta V)_{\rm s} \leqslant v_{\rm A}$) since the drain of energy from Alfvénic cascade is marginal when the amplitudes of perturbations become weaker. Most importantly in galaxy clusters it is $c_{\rm s}^2 \gg v_{\rm A}^2$ and thus the ratio between the amplitude of Alfvén and fast modes at scales $l < l_{\rm A}$ is expected to be small, $(\delta V)_c^2/(\delta\ V)_{\rm s}^2 \leqslant (v_{\rm A}/c_{\rm s})^2 \sim 10^{-2}$ (this for solenoidal forcing at $l \approx l_{\rm A}$).

3.4 Dissipation of turbulence in the ICM

3.4.1 Collisional regime and viscous dissipation

Viscosity is important in the dissipation of turbulent eddies in the collisional regime. In this regime the cascade of hydro-motions is maintained down to a scale $l_{\rm diss} \sim L_{\rm o}(Re)^{-3/4}$ at which the viscous dissipation rate equals the wave energy transfer rate. The damping rate of hydro-motions at scale l due to the viscosity is

$$\Gamma_k^{\nu} \sim \frac{\nu_{\rm K}}{l^2}. \tag{6}$$

Here $\nu_{\rm K}$ is a reference value of the kinetic viscosity which gives the main uncertainty in the calculations.

As a simplified and conservative approach we can assume that $\boldsymbol{B}_{\rm o}$ is initially ordered and that the first super-Alfvénic turbulent eddies, injected at large $L_{\rm o} \gg l_{\rm mfp}$ scales, initiate a cascading and thus that the bending of the field lines follows this cascading. Turbulent motions along $\boldsymbol{B}_{\rm o}$ experience the strongest viscous dissipation which can be grossly estimated by using the classical formulation of (unmagnetized) viscosity. By taking physical conditions appropriate for the central Mpc of hot galaxy clusters, the dissipation scale of these parallel motions reads

$$l_{\rm diss} \simeq l_{\rm mfp}\left(\frac{v_{\rm i}}{3V_{\rm L}}\right)^{3/4}\left(\frac{L_{\rm o}}{l_{\rm mfp}}\right)^{1/4} \approx l_{\rm mfp}\left(\frac{V_{\rm L}}{10^3\,{\rm km\,s^{-1}}}\right)^{-3/4}\left[\left(\frac{L_{\rm o}}{300\,{\rm kpc}}\right)\left(\frac{n_{\rm th}}{10^{-3}}\right)\left(\frac{8\,{\rm keV}}{T}\right)^{1/2}\left(\frac{\ln\Lambda}{40}\right)\right]^{1/4} \tag{7}$$

while turbulent motions transverse to $\boldsymbol{B}_{\rm o}$ experience a much smaller viscosity and shall cascade at scales $\ll l_{\rm mfp}$. The cascading of these transverse (quasi-perpendicular) motions at a given scale takes a time of the order of the bending time-scale of the magnetic field on the same scale and these motions become the responsible for the bending of the field lines on scales $\ll l_{\rm mfp}$, potentially down to scales $\approx l_{\rm A}$. We note that indeed recent *Bayesian* analysis of rotation measures show that magnetic fields in galaxy clusters could be tangled at least on scales $\approx$kpc (Vogt & Ensslin 2005), smaller scales being inaccessible to observations, thus suggesting that the bending of the field lines happens on scales $\ll l_{\rm mfp}$.

[3] The Alfvénic mode as well as the slow mode gets anisotropic for scales less than $l_{\rm A}$, which makes the scattering inefficient, however (Chandran 2000; Yan & Lazarian 2002).

As discussed in Section 3.2 the bending of the field lines on scales $<l_{\rm mfp}$ reduces the effective particle mean free path yielding a reduction of the viscosity. Viscosity indeed depends on the flux of the momentum which is transported by particles and this is determined by the diffusion of the particles that carry this momentum from the layers moving with different velocities. By limiting this diffusion the turbulent-bending of the field lines decreases the viscosity and thus the dissipation of turbulence itself.

Thus the turbulent eddies which cascade afterwards evolve in a very tangled magnetic field and experience an effective viscosity which we shall adopt in the form $\nu_{\rm K} \approx 1/3\ v_{\rm i} l_{\rm A}$, and the *effective* dissipation scale, $l^b_{\rm diss}$, we would encounter in the case of super-Alfvénic turbulent ICM becomes

$$l^b_{\rm diss} \approx l_{\rm diss}\left(\frac{l_{\rm A}}{l_{\rm mfp}}\right)^{3/4} \approx \frac{1}{45}\, l_{\rm mfp}\left(\frac{V_{\rm L}}{10^3\,{\rm km\,s^{-1}}}\right)^{-3}\left(\frac{L_{\rm o}}{300\,{\rm kpc}}\right)\left(\frac{B}{\mu{\rm G}}\right)^{9/4}\left(\frac{n_{\rm th}}{10^{-3}{\rm cm^{-3}}}\right)^{-1/8}\left(\frac{T}{8\,{\rm keV}}\right)^{-13/8}\left(\frac{\ln\Lambda}{40}\right). \quad (8)$$

Also in this case the effect driven by plasma instabilities in the ICM may affect our estimates. In particular, the scattering of thermal ions induced by these instabilities may additionally decrease the effective viscosity in the ICM, and this might reinforce our conclusions that, even assuming collisional physics, the bulk of compressible turbulent motions in the ICM is expected to be dissipated only at small scales, $\leqslant$ kpc.

3.4.2 Collisionless regime

The viscous damping is not important in the collisionless regime, that is, when the scales of interest are smaller than the particle's mean free path or when the time-scales of interest are shorter than the particle's collision time. When the diffusive-trajectory of particles is not driven only by collisions (as indeed in the super-Alfvénic turbulent-magnetized case, Sections 3.2 and 3.4.1) the most appropriate way to define the collisionless regime is in terms of collision frequency, and we shall use collisionless physics for the turbulent modes when the frequency of these modes is larger than the ion–ion collision frequency ν_{ii} (e.g. Eilek 1979):

$$\nu_{ii} \simeq \frac{4}{3}\sqrt{\pi}\frac{e^4 n_{\rm th}\ln(\Lambda)}{m_{\rm p}^{1/2}(k_{\rm B}T)^{3/2}}. \quad (9)$$

Magnetosonic modes dissipate energy in the collisionless regime in accelerating charged particles especially via TTD (e.g. Schlickeiser & Miller 1998) which is particularly severe in high-beta plasma conditions like those in the ICM. In terms of scales, from equation (9) and $\omega = V_{\rm ph}k$, the collisionless regime for magnetosonic waves in the ICM starts approximately at the scale of the ion mean free path $l_{\rm C} \sim l_{\rm mfp}$ (equation 1). Thus from a general point of view, in order to understand the way compressible modes dissipate in the ICM it is necessary to compare the viscous dissipation scale, $l^b_{\rm diss}$, with the collisionless scale $l_{\rm C}$: if $l^b_{\rm diss} < l_{\rm C}$ the cascading process of these turbulent modes would reach collisionless scales before being significantly affected by viscosity and energy will be dissipated via collisionless dampings, while in the opposite case turbulence will be dissipated by viscosity.

From equations (7) and (8) we immediately have that the bulk of compressive turbulence in the hot ICM is likely to be dissipated via collisionless dampings. Indeed in hot (and massive) galaxy clusters it is found that viscosity is not efficient enough to dissipate the turbulent motions, unless the large-scale velocity of these motions is relatively small, $V_{\rm L} < 300\,{\rm km\,s^{-1}}$, namely, in case of very low turbulence. At the same time, however, an efficient dissipation of turbulent motions may happen in strongly magnetized ($B \geqslant 5\,\mu$G), lower temperature and high density regions which are conditions appropriate at the centre of clusters with cooling flows (*cool cores*). Here viscosity may potentially become an important source of dissipation of the turbulent eddies.

It should be mentioned that plasma instabilities might complicate the picture. On one hand, their straightforward effect is to decrease the effective viscosity in the ICM, however, on the other hand they introduce a new relevant scattering frequency of ions which could be larger than the ion–ion scattering frequency (equation 9) and the net result might be that the collisionless regime gets into play at smaller scales. As in the previous sections we discard this possible effect which would deserve detailed investigation.

The nature (collisional or collisionless) of the turbulent dissipation in astrophysical plasma is a crucial point. In Table 1 we report the case for several astrophysical situations undertaking different physical conditions, processes and scales of interest. A collisionless dissipation

Table 1. The reference parameters of astrophysical plasma and relevant damping. The dominant damping mechanism for turbulence is given in the last line. GC = hot galaxy clusters, CC = cool-cluster cores, HIM = hot ionized ISM, WIM = warm ionized ISM, SUN = solar flare plasma.

	GC	CC	Galactic halo	HIM	WIM	Sun
T (K)	10^8	3×10^7	2×10^6	10^6	8×10^3	10^7
$c_{\rm s}$ (km s^{-1})	1650	900	130	90	8	360
$n_{\rm th}$ (cm^{-3})	10^{-3}	5×10^{-2}	10^{-3}	4×10^{-3}	0.1	10^{10}
$l_{\rm mfp}$ (cm)	5×10^{22}	10^{20}	4×10^{19}	2×10^{18}	6×10^{12}	10^8
$L_{\rm o}$ (pc)	1–5×10^5	1–5×10^5	100	100	50	3×10^{-10}
B (μG)	1	10	5	2	5	10^8
$c_{\rm s}^2/v_{\rm A}^2$	500	100	0.3	3.5	0.1	0.03
Damping	*Collisionless*[a]	*Collisionless*?	*Collisionless*	Collisional	Collisional	*Collisionless*[b]

[a] $V_{\rm L} > 300\,{\rm km s^{-1}}$. [b] Alfvénic turbulent-Mach number $M_{\rm A} \geqslant 0.3$ is assumed.

of compressive turbulence is believed to be eventually operating in a few other astrophysical regions such as in solar flare plasma and in the Galactic halo. It is important to note here that stochastic particle acceleration is indeed suggested to power the hard X-ray flares observed in the Sun (e.g. Miller, La Rosa & Moore 1996; Petrosian, Yan & Lazarian 2006). We note that the beta of plasma in these filaments is extremely small and thus even in the case of strong turbulence the collisionless dissipation of compressive modes should happen at scales, $l \leqslant l_{\rm A}$, at which turbulent motions are MHD in nature. On the other hand turbulence in the ICM is super-Alfvénic (essentially due to the high beta of plasma) and the collisionless regime in the hot ICM starts at scale $l > l_{\rm A}$ were compressive motions are still hydro in nature.

3.5 Conclusion I: turbulent scenario in the ICM

Given the above discussions it is possible to set up a simplified and operative scenario of turbulence in the ICM to adopt in this paper.

Within a simplified picture of turbulence that we consider here, super-Alfvénic turbulence is made by a mix of magnetosonic modes (essentially similar to sound modes) and incompressible-Kolmogorov turbulent eddies (which roughly correspond to the Alfvén modes in the MHD regime).

We shall assume that turbulence is injected at large scales $L_{\rm o} \sim$ 300–500 kpc most likely by a complex mixture of compressive and solenoidal forcing. The typical velocity of the turbulent eddies at the injection scale is expected to be around $V_{\rm L} \sim$ 500–1000 km s^{-1} which makes turbulence subsonic, with $M_{\rm s} = V_{\rm L}/c_{\rm s} \approx 0.3$–$0.8$, but strongly super-Alfvénic, with $M_{\rm A} = V_{\rm L}/v_{\rm A} \geqslant 10$. Turbulent motions at large scales are thus essentially hydrodynamics and the cascading of compressive (magnetosonic) modes may couple with that of solenoidal motions (Kolmogorov eddies).

Assuming typical conditions in hot (and massive) galaxy clusters we find that even in the unmagnetized case viscosity would still allow hydro-motions to cascade down to scales of the order of $\approx l_{\rm mfp}$. In the magnetized case viscosity is believed to be partially suppressed. In addition, when turbulence is super-Alfvénic hydro-motions can easily bend the magnetic field lines affecting the *effective* mean free path of ions which happens to become limited approximately to the MHD scale, $l_{\rm A}$.[4] The value of the effective viscosity, even for motions along the magnetic field lines, is thus expected to be considerably reduced with respect to the classical unmagnetized value and one may adopt a reasonable value of the Reynolds number $Re \geqslant 10^3$.

The important consequence of this picture is that both solenoidal and compressive modes in hot galaxy clusters would not be strongly affected by viscosity at large scales and an inertial range is established, provided that the velocity of the eddies at large scales exceeds $\approx$300 km s^{-1}. We shall assume that a sizeable part of the large-scale turbulence is done by magnetosonic (essentially sound) modes. At collisionless scales, $l <$ 10–50 kpc, these modes are affected by strong collisionless dampings with both thermal and relativistic particles (Section 4.3) and thus they are expected to be the modes which dominate the particle acceleration process. Our claim about the existence of this well developed turbulent cascade which establishes an inertial range from large scales to the collisionless scales would be even reinforced when the possible effect of plasma instabilities is considered.

Although in this paper we focus on the particle acceleration by hydro-magnetosonic modes, it is worth mentioning that the mode composition at smaller scales, $l \ll l_{\rm A}$, in the ICM should becomes much complex. We shall assume that Alfvén modes are present at these MHD scales in the ICM since in principle the cascading of solenoidal modes might reach very small scales, due to the lack of large-scale collisionless dampings for these modes, and also because several mechanisms can convert a fraction of the energy flux of large-scale turbulent cascade in the injection of Alfvén modes at smaller scales (e.g. Kato 1968; Eilek & Henriksen 1984; Lazarian & Beresnyak 2006). At scales $l \leqslant l_{\rm A}$, the coupling between Alfvén and compressible modes gets changed and only slow modes are cascaded by Alfvénic modes (GS95, Lithwick & Goldreich 2001; Cho & Lazarian 2002), while the cascading of fast modes is not particularly sensitive to the presence of the other modes. Given that, and since magnetosonic modes are expected to be damped at scales larger than (or similar to) $l_{\rm A}$ (Sections 4 and 5), the spectrum of the ICM-turbulence at $l \ll l_{\rm A}$ is expected to be populated only by Alfvén and slow modes. These modes however would get anisotropic at these scales (unless injected at these scales by some mechanism) and this should reduce their contribution to the scattering and acceleration of fast particles via gyroresonance.

4 COMPRESSIBLE TURBULENCE IN THE COLLISIONLESS REGIME

Compressible turbulence in galaxy clusters is thus made of large-scale hydro-motions with frequencies essentially *infinitely* small with respect to $\Omega_{\rm i}/\beta_{\rm pl}$ ($\Omega_{\rm i}$ being the Larmor frequency of ions). The basic physics of these low-frequency compressible modes in the collisionless regime can be derived by mean of the quasi-linear theory and has been investigated in several seminal papers (e.g. Barnes 1968; Melrose 1968; Baldwin, Bernstein & Weenink 1969; Barnes & Scargle 1973, hereafter BS73).[5] This section extends previous studies as we derive specific and operative expressions for the physical properties of these modes which are of interest for the present paper (e.g. energy decomposition of the mode, TTD-damping rate) and discuss their dependence on the mode-propagation angle. We focus on the case of long-wavelength modes in a magnetized plasma dominated by thermal particles as it should be the case of the ICM. Here we report the main formulae, while details and derivation of the main equations are given in Appendices A–C.

[4] This provided that turbulent eddies may reach the MHD scale without being dissipated (Sections 5.1.3 and 5).

[5] For hydromagnetic waves with frequency of the order of $\Omega_{\rm i}/\beta_{\rm pl}$ see Foote & Kulsrud (1979).

4.1 Geometry of the mode and dielectric tensor

We define the turbulent fluctuations associated with the electric and magnetic field as

$$\boldsymbol{E} = \mathcal{R}\left(\boldsymbol{E}_k \exp[\mathrm{i}(\boldsymbol{k}\cdot\boldsymbol{r} - \omega t)]\right) \tag{10}$$

and

$$\boldsymbol{B} = \mathcal{R}\left(\boldsymbol{B}_k \exp[\mathrm{i}(\boldsymbol{k}\cdot\boldsymbol{r} - \omega t)]\right), \tag{11}$$

where $\mathcal{R}()$ stands for the real part. In the collisionless regime it is usual to start with fixing the geometry of the mode propagation and of the electric field fluctuations. Without loss of generality we may chose the particular system where the y-component of the wavevector of the modes vanishes, that is,

$$\boldsymbol{k} = (k_\perp, 0, k_\parallel). \tag{12}$$

For this choice the amplitude of the electric field (and spatial Fourier transform of the electric field of the mode) is given by (e.g. BS73)

$$\boldsymbol{E}_k = (0, E_\perp, E_\parallel). \tag{13}$$

The amplitude of the magnetic field of the mode comes from the Faraday law, $\boldsymbol{B}_k = \frac{c}{\omega}\boldsymbol{k}\times\boldsymbol{E}_k$:

$$\boldsymbol{B}_k = \frac{c}{\omega}(-k_\parallel E_\perp, -k_\perp E_\parallel, k_\perp E_\perp). \tag{14}$$

As a starting point we assume the presence of several, α, species of particles with particle momentum given by

$$\boldsymbol{p}_\alpha = (p_\perp\cos\phi,\, p_\perp\sin\phi,\, p_\parallel) = m_\alpha\gamma(v_\perp\cos\phi,\, v_\perp\sin\phi,\, v_\parallel) \tag{15}$$

and indicate with $\hat{f}_\alpha$ the normalized particle distribution in the momentum space of species α ($f_\alpha(p) = N_\alpha\hat{f}_\alpha(p)$).

The properties of a wave propagating in a magnetized plasma in the collisionless regime depend on the dielectric tensor of the plasma. In the general case, the dielectric tensor of the magnetized plasma is given by (e.g. Melrose 1968; see also Tsytovich 1977 for the unmagnetized case):

$$K_{ij} = \delta_{ij} + 2\pi\sum_\alpha m_\alpha\left(\frac{\omega_{\mathrm{p},\alpha}}{\omega}\right)^2\int\int \mathrm{d}p_\perp p_\perp \mathrm{d}p_\parallel\left[\frac{v_\parallel}{v_\perp}\left(v_\perp\frac{\partial}{\partial p_\parallel} - v_\parallel\frac{\partial}{\partial p_\perp}\right)\hat{f}_\alpha(p) b_i b_j + \sum_{n=-\infty}^{\infty}\frac{\left(V_i V_j^*\right)_\alpha}{\omega - n\Omega_\alpha - k_\parallel v_\parallel}\right.$$
$$\left.\times\left(\frac{\omega - k_\parallel v_\parallel}{v_\perp}\frac{\partial}{\partial p_\perp} + k_\parallel\frac{\partial}{\partial p_\parallel}\right)\hat{f}_\alpha(p)\right], \tag{16}$$

where $\omega_{\mathrm{p},\alpha} = \sqrt{4\pi N_\alpha e_\alpha^2/m_\alpha}$ is the plasma frequency for the species α, $b_i = (\boldsymbol{B}_\mathrm{o}/|B_\mathrm{o}|)_i$ is the unit vector along the magnetic field, $\Omega_\alpha = (e_\alpha B_\mathrm{o}/m_\alpha c)/\gamma$ is the Larmor frequency of particles α,

$$\left(V_i V_j^*\right)_\alpha = \begin{pmatrix} \left(\frac{v_\perp n}{z}\right)^2 J_n^2(z) & \mathrm{i}\frac{v_\perp^2 n}{z}J_n(z)J_n'(z) & \frac{v_\perp v_\parallel n}{z}J_n^2(z) \\ -\mathrm{i}\frac{v_\perp^2 n}{z}J_n(z)J_n'(z) & v_\perp^2(J_n'(z))^2 & -\mathrm{i}v_\perp v_\parallel J_n(z)J_n'(z) \\ \frac{v_\perp v_\parallel n}{z}J_n^2(z) & \mathrm{i}v_\perp v_\parallel J_n(z)J_n'(z) & v_\parallel^2 J_n^2(z) \end{pmatrix}_\alpha \tag{17}$$

and $z_\alpha = k_\perp p_\perp/m_\alpha\Omega_\mathrm{o}^\alpha$ ($\Omega_\mathrm{o}^\alpha = \Omega\gamma$ is the classical Larmor frequency) is an adimensional parameter which scales with the ratio between the frequency of the mode and the particle Larmor frequency, and with the ratio between the particle velocity and the phase velocity of the mode, $z_\alpha \approx (\omega/\Omega_\mathrm{o}^\alpha)(v_\alpha/V_\mathrm{ph})$. We notice that magnetosonic modes with long wavelength, $l \gg$ pc, always have $z_\alpha \ll 1$. In this case a more suitable expression for the dielectric tensor can be obtained by expanding the *Bessel functions* in equations (16) and (17) in the limit $z_\alpha \ll 1$ (Appendix A).

4.2 Energy of the mode

The energy of a mode in a magnetized plasma is done by the sum of the energy associated with the fluctuations of the electric and magnetic fields, W_E and W_B, and by the energy contributed by particles to the modes, W_P. The total energy is then

$$W = W_\mathrm{B} + W_E + W_P. \tag{18}$$

In the collisional regime (and adiabatic equation of state) W_P is given by the contributions from the kinetic energy, W_K, and from a potential energy, W_Φ, associated with pressure fluctuations, and a simple equipartition condition exists (e.g. Denisse & Delcroix 1963; Melrose 1968), namely,

$$W_\mathrm{B} + W_\Phi \approx W_E + W_\mathrm{K}. \tag{19}$$

In the collisionless regime the medium is described in terms of the dielectric tensor and it is not possible to define W_P in a meaningful way. Thus one has to use equation (18) as a definition for W_P, with the total energy, W, defined independently. The total energy of the mode is given by (e.g. Barnes 1968; see also Melrose 1968; Tsytovich 1972 for equivalent expressions)

$$W(k,\omega) = \frac{1}{16\pi}\left[B_{k\,i}^* B_{k\,i} + E_{k\,i}^*\frac{\partial}{\partial\omega}\left(\omega K_{ij}^\mathrm{h}\right)E_{k\,j}\right]_{\omega_\mathrm{i}=0}, \tag{20}$$

where $K^{\rm h}_{ij}$ stands for the Hermitian part of the dielectric tensor. In this case the first term in equation (20) accounts for magnetic field fluctuations, while (from equation 18) the term

$$\frac{1}{16\pi}\left[E_{k\,i}^{*}\frac{\partial}{\partial\omega}\left(\omega K^{\rm h}_{ij}\right)E_{k\,j}\right]=\frac{|E_k|^2}{16\pi}+\sum_{\alpha}[W_P(k)]_{\alpha} \tag{21}$$

accounts for the contribution to the mode energy from the electric field fluctuations and from particles (Barnes 1968).

In the quasi-linear regime the energy of the magnetic field fluctuations is related to that of electric field fluctuations by (e.g. Melrose 1968):

$$W_{\rm B}=\left(\frac{c}{V_{\rm ph}}\right)^2\left(1-\left|\frac{\boldsymbol{k}}{k}\cdot\frac{\boldsymbol{E}_k}{|E_k|}\right|^2\right)W_E \tag{22}$$

which can be taken $W_{\rm B}\simeq(c/V_{\rm ph})^2W_E$ since under the physical conditions of interest for this paper magnetosonic modes have $E_\perp/E_\parallel\ll 1$ (Appendix B). Thus combining equation (18) with equations (20)–(22) it is easy to get the ratio between the total energy in the mode and that associated with the different components, $W_{\rm B}$, W_E and W_P.

Thermal particles in the ICM should provide the dominant contribution to the total energy of turbulent modes. Thus we make the approximation that the dielectric tensor of the ICM is described by that of an electron–proton magnetized plasma in thermal equilibrium. Assuming a Maxwellian distribution for the thermal electrons and protons in the ICM:

$$f_\alpha(p)=N_\alpha\hat{f}_\alpha(p)=\frac{N_\alpha}{(2\pi m_\alpha k_{\rm B}T)^{3/2}}\exp\left(-\frac{p^2}{2m_\alpha k_{\rm B}T}\right) \tag{23}$$

in Appendix B, from equations (16), (17) and (20) we show that the total energy of a fast mode is

$$W(k,\theta)=\frac{|B_k|^2}{16\pi}\left\{1+\frac{\beta_{\rm pl}}{2}\left[\left(\frac{V_{\rm ph}}{c_{\rm s}}\right)^2+\frac{3}{5}\left(\frac{k_\perp}{k}\right)^2(2-\mathcal{S}(\beta_{\rm pl},\theta))+\frac{1}{\beta_{\rm pl}}\left(\frac{V_{\rm ph}}{c}\right)^2\left(\frac{3}{5}\beta_{\rm pl}+2\right)\right]\right\}, \tag{24}$$

where the function $\mathcal{S}(\beta_{\rm pl},\theta;\{f_{\rm rel}(p),T\})$ (Fig. 1) accounts for the terms of the dielectric tensor in the form

$$\int {\rm d}p_\parallel {\rm d}p_\perp p_\perp^m\frac{\partial f_\alpha/\partial p_\parallel}{k_\parallel v_\parallel-\omega} \tag{25}$$

which all come from the collisionless resonance between particles and modes with $n=0$ in equation (16) (see Section 5.1 and Appendix B). Provided f_α is an even function of $p_\parallel$, only particles with velocity larger than the phase velocity of the mode can contribute to $\mathcal{S}$, since they should satisfy the condition $k_\parallel v_\parallel\sim\omega=V_{\rm ph}k$. The velocity of the selected resonant particles scales as $v\sim V_{\rm ph}(\beta_{\rm pl})/\cos(\theta)$, thus with increasing the angle between $\boldsymbol{k}$ and $B_{\rm o},\theta$, particles with increasing velocities may contribute to this term. Formally particles with $v\to\infty$ contribute to $\mathcal{S}$ for $\theta\to\pi/2$, and this gets $\mathcal{S}\to 0$ in this limit (Fig. 1). Two *wave-like behaviour* of $\mathcal{S}$ can be recognized in Fig. 1: the first one, for $\theta\leqslant 1$, marks the contribution from protons, while the second one, for larger θ, marks that from electrons, which are faster than protons. The resonance condition, $k_\parallel v_\parallel\sim\omega$, also drives the shift of these *wave-like behaviour* towards smaller values of θ with decreasing $\beta_{\rm pl}$: when $\beta_{\rm pl}$ decreases the resonance between the mode and a fixed portion of the particle distribution comes up at smaller values of θ.

In Fig. 2 we report the ratio between magnetic and total energy of a mode propagating at an angle θ as a function of $\beta_{\rm pl}$; this ratio is independent of the wavenumber k of the mode. Two *wave-like behaviours* (due to the contribution from $\mathcal{S}$-terms) are visible: the first one, for

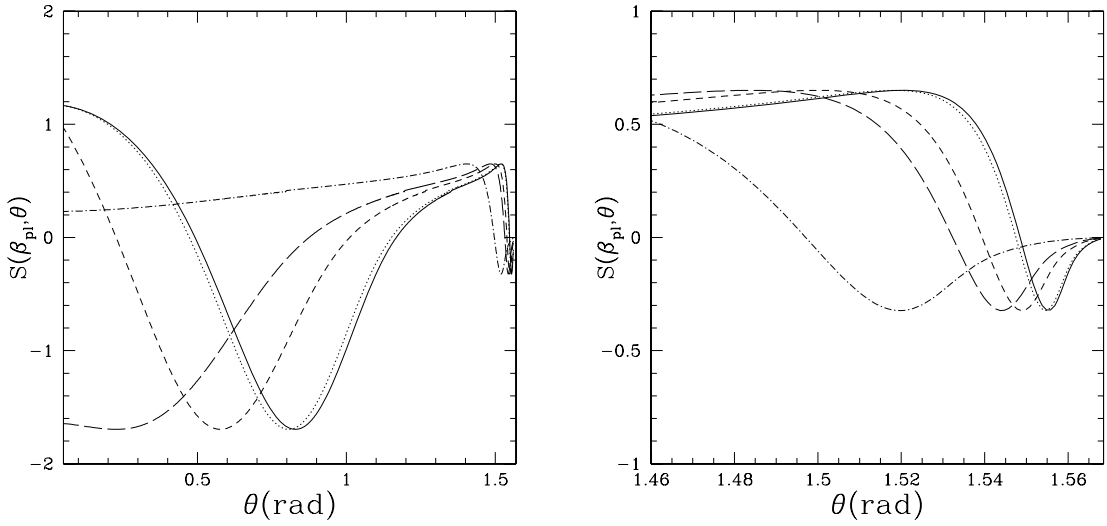

Figure 1. (a) The expression $S(\beta_{\rm pl},\theta)$ is given as a function of θ. The behaviour around $\theta=\pi/2$ is highlighted in the right-hand panel. $k_{\rm B}T=8.6$ keV is assumed. Calculations are reported for: $c_{\rm s}^2/v_{\rm A}^2=\beta_{\rm pl}/2=100$ (solid line), 10 (dotted line), 1 (dashed line), 0.5 (long-dashed line) and 0.1 (dash–dotted line).

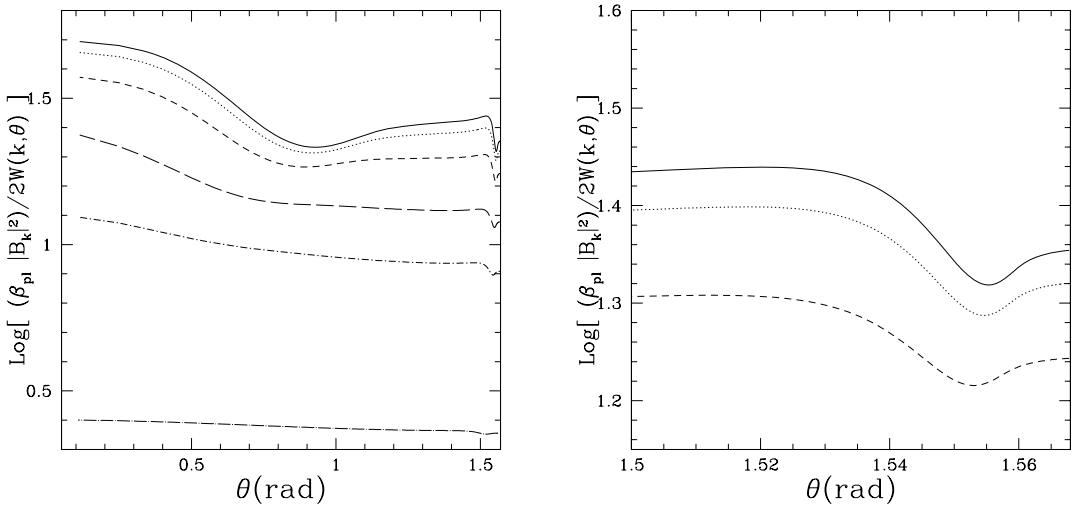

Figure 2. The ratio between the magnetic energy density of the mode and the total energy density of the mode is given as a function of θ (for a better comparison the quantity is multiplied by $16\pi\,\beta_{\rm pl}/2$). The behaviour around $\theta = \pi/2$ is highlighted in the right-hand panel. $k_{\rm B}T = 8.6$ keV is assumed. Calculations are reported for: $c_{\rm s}^2/v_{\rm A}^2 = \beta_{\rm pl}/2 = 100$ (solid line), 10 (dotted line), 3 (dashed line), 1 (long-dashed line), 0.5 (short-dashed–dotted line) and 0.1 (long-dashed–dotted line).

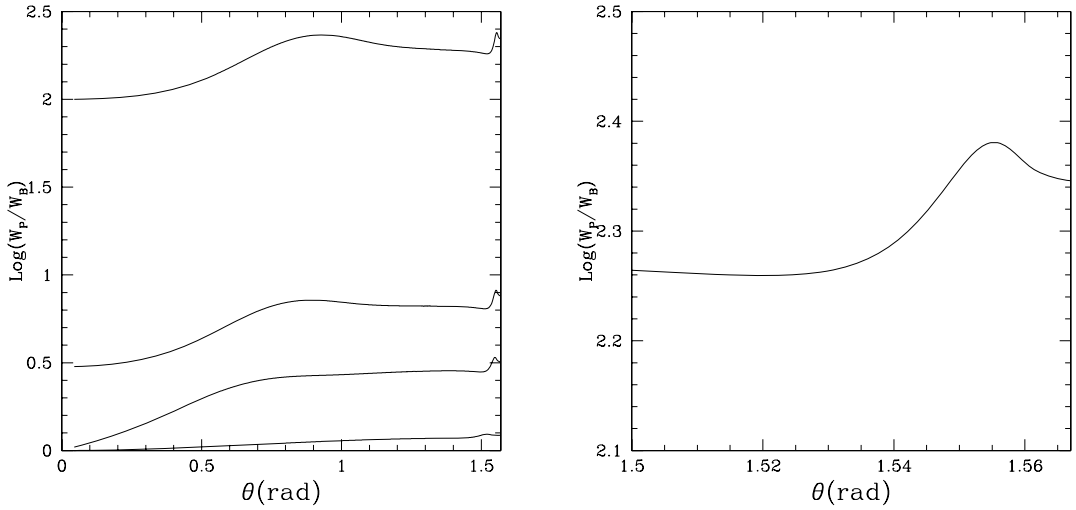

Figure 3. The ratio between particle energy and magnetic energy in the mode is reported as a function of θ; $k_{\rm B}T = 8.6$ keV is assumed. Calculations are reported for: $c_{\rm s}^2/v_{\rm A}^2 = 0.1$, 1, 3 and 100 (from the bottom to the top of the diagram). The behaviour at $\theta \sim \pi/2$ is highlighted in the right-hand panel for $c_{\rm s}^2/v_{\rm A}^2 = 100$.

$\theta \leqslant 1$, marks the contribution from protons, and the second one, for larger θ, from electrons. For small values of $\beta_{\rm pl}$ it is $W_{\rm B} \approx W/2$ and thus the quantity $\beta_{\rm pl}|B_k|^2/2W \propto \beta_{\rm pl}$, on the other hand, for large values of $\beta_{\rm pl}$ it is $W_{\rm B} \propto W/\beta_{\rm pl}$ and $\beta_{\rm pl}|B_k|^2/2W$ becomes independent of $\beta_{\rm pl}$.

Finally, in Fig. 3 we report the ratio between particle energy and magnetic energy in the mode for different values of $\beta_{\rm pl}$ (see caption). For $\beta_{\rm pl} \ll 1$, W_P reaches equipartition with $W_{\rm B}$ similarly to the case of collisional and low $\beta_{\rm pl}$ plasmas.

4.3 Turbulence damping: TTD resonance ($n = 0$)

A compressible mode in the collisionless regime experiences strong collisionless damping with thermal and relativistic particles and gets modified. In this section we report relevant formulae for the collisionless damping rate via TTD resonance of magnetosonic waves which will be used in the present paper (Section 5).

The damping coefficient of the mode can be obtained by the standard formula for the linear growth rate of the mode in the quasi-linear theory (e.g. BS73)[6]:

$$\Gamma = -{\rm i}\left(\frac{E_i^* K_{ij}^a E_j}{16\pi W}\right)_{\omega_{\rm i}=0} \omega_{\rm r}, \tag{26}$$

[6] With this formula it is $\partial W/\partial t = -\Gamma W$.

where K^a_{ij} stands for the anti-Hermitian part of the dielectric tensor, and ω_r is the real part of ω. The general formula for the collisionless damping rate ($n = 0, \pm1, \ldots$) is (Appendix C, and BS73):

$$\Gamma(k,\theta) = -\frac{\pi}{16\omega_r W(k,\theta)}\frac{k_\parallel}{|k_\parallel|}\sum_{\alpha,n}\omega^2_{p,\alpha}\int_0^\infty \mathrm{d}p_\perp \int_{-\infty}^{\infty}\mathrm{d}p_\parallel p_\perp^2 \Psi_n^\alpha \left[\left(\frac{\omega}{k_\parallel}-v_\parallel\right)\frac{\partial \hat{f}_\alpha(p)}{\partial p_\perp}+v_\perp\frac{\partial \hat{f}_\alpha(p)}{\partial p_\parallel}\right]\ \delta\left(\frac{p_\parallel}{m_\alpha}+\frac{n\Omega_{o,\alpha}-\omega_r\gamma}{k_\parallel}\right), \tag{27}$$

where

$$\Psi_n^\alpha = 2\left|\mathrm{i}J_n'(z_\alpha)E_\perp+\frac{p_\parallel}{p_\perp}J_n(z_\alpha)E_\parallel\right|^2. \tag{28}$$

In this paper we focus on the case $n = 0$ (TTD, discussed in Section 5) which is the most important collisionless resonance between magnetosonic waves and particles in the ICM. In the case of long-wavelength magnetosonic waves the damping rate due to TTD resonance with thermal electrons and protons with number density $N_{e/p}$, is given by (Appendix C)

$$\Gamma_{e/p}(k,\theta) = \sqrt{\frac{\pi}{8}}\frac{|B_k|^2}{W(k,\theta)}\mathcal{H}\left(1-\frac{V_{ph}}{c}\frac{k}{|k_\parallel|}\right)\frac{V_{ph}^2}{B_o^2}\left(\frac{k}{|k_\parallel|}\right)\left(\frac{k_\perp}{k}\right)^2\frac{(m_{e/p}k_B T)^{1/2}}{1-[V_{ph}k/(ck_\parallel)]^2}N_{e/p}\exp\left\{-\frac{m_{e/p}V_{ph}^2}{2k_B T}\frac{(k/k_\parallel)^2}{1-[V_{ph}k/(ck_\parallel)]^2}\right\}k, \tag{29}$$

where $\mathcal{H}(x)$ is the Heaviside step function (1 for $x > 0$, and 0 otherwise), and the ratio $|B_k|^2/W$ is given by equation (24).

Actually for a fixed value of β_{pl}, the damping rate scales with $\sqrt{T}$ and this makes the damping strong in the case of galaxy clusters ($T \sim 10^7$–10^8 K). For $\beta_{pl} \gg 1$ the TTD-damping rate from thermal electrons is $\Gamma_e/\omega_r \approx \sqrt{3\pi x/20}\exp(-5x/3)\sin^2\theta$, where $x = (m_e/m_p)/\cos^2\theta$, which is sufficiently small[7] to make the linear-theory approach adopted here still reasonable. Equation (29) is a general expression of the damping rate due to TTD resonance with thermal particles from which well-known formulae can be readily re-obtained. For instance in the case of low β_{pl} it is $V_{ph} \to v_A$ and $(|B_k|^2/16\pi W) \to 1/2$ and one gets the usual TTD-damping rate of fast modes with thermal electrons (e.g. Akhiezer et al. 1975; Achterberg 1981; Miller 1991):

$$\Gamma_{e/p}(k,\theta) \to \sqrt{\frac{\pi}{2}}\frac{m_e}{m_p}\frac{v_{te}}{v_A}\frac{\sin^2\theta}{|\cos\theta|}\exp\left(-\frac{v_A^2}{2v_{te}^2\cos^2\theta}\right)v_A k, \tag{30}$$

where we define $v_{te} = \sqrt{k_B T/m_e}$. A formula equal to equation (30) is also given for $\beta_{pl} \ll 1$ in Ginzburg (1961) and Shafranov (1967) without adopting the simplified quasi-linear approach. These authors also report a non-quasi-linear formula for the damping rate of thermal electrons and protons under the *particular* condition of $c_s \ll V_{ph} \ll v_{te}$, in which case the plasma dielectric tensor can be largely simplified by expanding the *Z-function* (Appendix B, equations B17–B18) of electrons and protons for large (protons) and small (electrons) arguments. In this case the normalization of the formula for the damping rate of protons is five times larger than that in equation (30), while the formula for the damping of electrons is equal to equation (30) (this *asymmetry* in the electron–proton contribution comes from the expansions of the *Z-function* in the two opposite regimes for electrons and protons). Still since it is $c_s \ll V_{ph}$ the damping from protons is negligible and equation (30) is equivalent to the result reported by these authors.

The damping rate due to ultrarelativistic electrons and protons is given by (Appendix C, and BS73):

$$\Gamma_{e/p}(k,\theta) = -\frac{\pi^2}{8}\frac{|B_k|^2}{W(k,\theta)}\left(\frac{k_\perp}{k}\right)^2\left(\frac{k}{|k_\parallel|}\right)\mathcal{H}\left(1-\frac{V_{ph}}{c}\frac{k}{|k_\parallel|}\right)\frac{N_{e^\pm/p}\ V_{ph}^2}{B_o^2}\ k\left[1-\left(\frac{V_{ph}k}{ck_\parallel}\right)^2\right]^2\int^\infty p^4\mathrm{d}p\left[\frac{\partial \hat{f}_\alpha(p)}{\partial p}\right]_{e/p}, \tag{31}$$

while the damping rate due to generic non-ultrarelativistic and non-thermal particles is given in Appendix C (equation C9).

In Fig. 4 we report the damping rate from both thermal and relativistic particles under conditions typical of massive and hot galaxy clusters. The most important damping for a mode propagating at small angles ($\theta \leqslant 1$) is that with thermal protons, on the other hand, a mode propagating at larger angles is damped by thermal electrons. We find that under viable physical conditions the damping due to relativistic particles is formally relevant only in a narrow range of the values of θ (close to $\theta \sim \pi/2$), and that it accounts for only a few per cent of the total damping rate.

For a given temperature of the plasma, T, the strength of the damping rate decreases with decreasing β_{pl} as the phase velocity of the modes increases with respect to the thermal velocity and this makes the particle-mode resonance more difficult.

We notice that the overall damping rate is anisotropic with a relatively narrow peak at $k/k_\parallel \sim 30$ (for high β_{pl}) where the bulk of thermal electrons resonates with the modes. On the other hand, as discussed in Section 3, the ICM turbulence is super-Alfvénic and thus the turbulent modes can easily bend the magnetic field lines. The time-scale of the bending of lines from hydro-motions on a scale l is expected to be $\approx$ a fraction of l/v_l, where v_l is the rms velocity of the turbulent eddies at the scale l. The bending of the lines by hydro-motions on the shortest scales is thus the most efficient so that we can grossly estimate this bending time-scale, τ_{bb}, as $\approx$ a fraction of l_A/v_A; eddies on scales below l_A cannot significantly bend the field lines.[8] This value of τ_{bb} should be compared with that of the damping time at collisionless scales which is grossly (from equations 29 and 24) $\Gamma(k)^{-1}(l_{mfp}) \approx \sqrt{m_p/m_e}l_{mfp}/c_s$. The relevant time-scale for isotropization of the pitch angle θ due to

[7] Γ_e/ω_r has a maximum value $\approx$0.2.

[8] The wandering of the magnetic field at scales $l \leqslant l_A$ is discussed in Yan & Lazarian (2004).

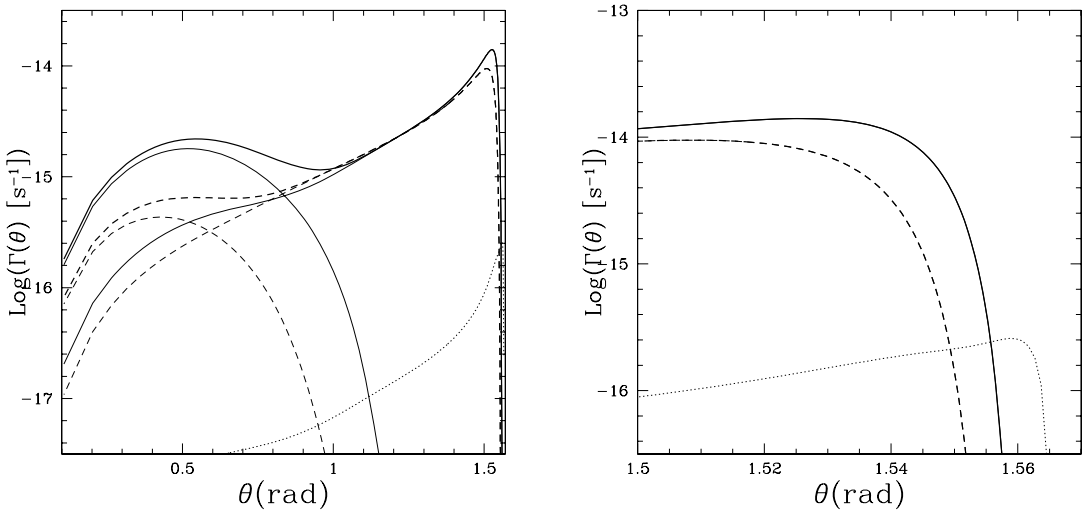

Figure 4. The damping rates of magnetosonic modes due to TTD resonance with thermal electrons (upper curves in the right-hand end of the panel) and with thermal protons (upper curves in the left-hand end of the panel), and the total damping rate (thick curves) are reported as a function of θ. The behaviour at about $\theta = \pi/2$ is highlighted in the right-hand panel. Calculations are reported for: $c_s^2/v_A^2 = 100$ (solid lines) and 1 (dashed lines), and taking $k = 1$ kpc^{-1} and $k_B T = 8.6$ keV. The damping rate with relativistic protons is also reported in both panels (dotted lines): in this case we assume an energy distribution in the form $f(p) \propto p^{-4.2}$ and an energy density ∼5 per cent of the thermal one.

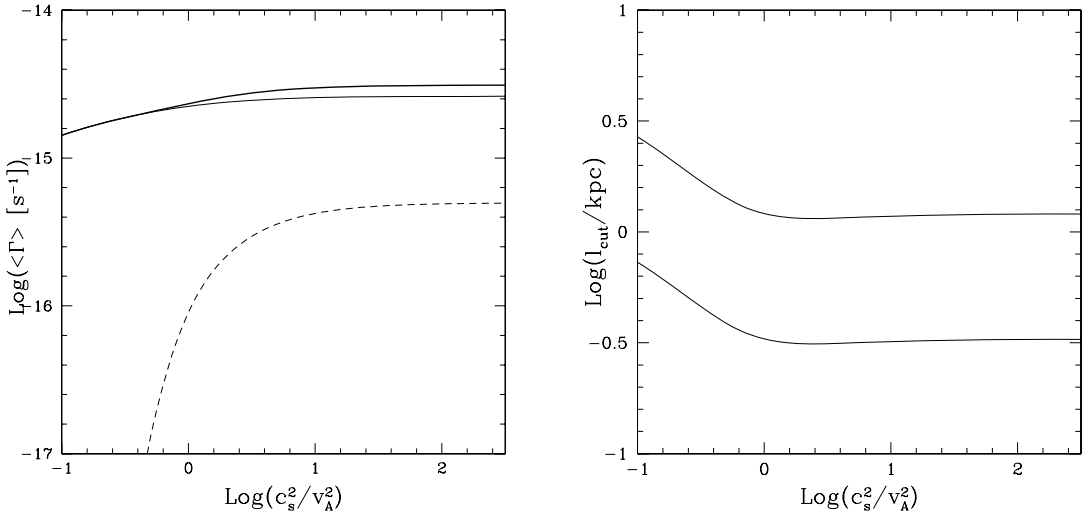

Figure 5. (a) The average damping rates of magnetosonic modes (equation 33), due to TTD resonance with thermal electrons (solid line) and thermal protons (dashed lines), and total damping rate (thick solid line) are reported as a function of $c_s^2/v_A^2 (= \beta_{pl}/2)$; $k = 1$ kpc^{-1} is taken. (b) The turbulent cut-off scale (equation 45) is reported as a function of c_s^2/v_A^2 $(= \beta_{pl}/2)$. Calculations are obtained assuming $L_o = 300$ kpc, and $(V_L/c_s)^2 = 0.15$ (upper curve) and $(V_L/c_s)^2 = 0.3$ (lower curve). In both panels we assume $k_B T = 8.6$ keV.

line-bending is thus faster than the damping process, that is, $\tau_{bb} < 1/\Gamma(l_{mfp})$, in the case[9]

$$\beta_{pl} \gg \left(\frac{L_o}{l_{mfp}}\right)\left(\frac{V_L}{c_s}\right)^{-3}\left(\frac{m_e}{m_p}\right)^{1/2}. \quad (32)$$

The condition in equation (32) is always satisfied in the ICM, at least under the hypothesis of this paper, and thus we shall use an effective damping rate *for the bulk of the spectrum* of magnetosonic modes which comes from the contribution from different θs and is defined by

$$\langle \Gamma_{e/p}(k) \rangle = \int_0^{\pi/2} \Gamma_{e/p}(k, \theta) \sin\theta \, d\theta. \quad (33)$$

This is reported in Fig. 5(a) as a function of c_s^2/v_A^2 $(= \beta_{pl}/2)$ (for a given temperature of the ICM, see caption). Damping of magnetosonic modes is found to be always dominated by thermal electrons because they are faster than the phase velocity of these modes. The contribution

[9] Here we assume that turbulent eddies reach scales $\leqslant l_A$ (Section 5.1.3, Fig. 6a), in case $l_{cut} \geqslant l_A$ the bending time-scale gets grossly of the order of a fraction of the damping time-scale at the cut-off scale, which would still be sufficient to have some isotropization.

from thermal protons drops for $\beta_{\rm pl} \leqslant 20$ since for smaller beta the phase velocity of the modes (equation 4) increases with respect to the proton velocity and it is even more difficult for protons to satisfy the resonant condition.

Finally, let us comment that it is $\langle\Gamma\rangle/\omega_{\rm r} \ll 1$ and this further motivate the practical use of the quasi-linear theory in this paper.

5 STOCHASTIC PARTICLE ACCELERATION IN GALAXY CLUSTERS

In this section we discuss the particle acceleration process in the ICM via resonant and non-resonant mechanisms with compressible modes.

5.1 Resonant TTD-acceleration

5.1.1 Introduction

Compressible (and incompressible) low-frequency MHD waves can strongly affect particle motion through the action of the mode-electric field via gyroresonant interaction (e.g. Melrose 1968), the condition for which is

$$\omega - k_{\parallel} v_{\parallel} - n\frac{\Omega}{\gamma} = 0, \tag{34}$$

where $n = \pm 1, \pm 2, \ldots$ gives the first (fundamental), second, ... harmonics of the resonance, while $v_{\parallel} = \mu v$ and $k_{\parallel} = \eta k$ are the parallel (projected along $B_{\rm o}$) speed of the particles and the wavenumber, respectively. In general gyroresonance is a process important only for modes at very small scales, $l \ll l_{\rm A}$. However, as anticipated in Section 3.5, at these scales fast modes are probably absent in the ICM due to strong resonant dampings (Section 5.1.3, Figs 4–6) and because they do not couple with the Alfvénic cascade (Sections 3.3.2 and 3.5).

Interestingly enough, the compressible component of the magnetic field of compressible modes (i.e. the component along $\boldsymbol{B}_{\rm o}$ in the case of oblique propagation) can interact with particles through

the $n = 0$ resonance. This interaction is called *transit-time damping* (e.g. Fisk 1976; Eilek 1979; Miller et al. 1996; Schlickeiser & Miller 1998). An important aspect of this interaction is the need of isotropization of particle momenta during acceleration (e.g. Schlickeiser & Miller 1998). This is because the $n = 0$ resonance changes only the component of the particle momentum parallel to the seed magnetic field. This would cause an increasing degree of anisotropy of the particle distribution and thus the deriving acceleration would become less and less efficient with time. Under our working picture, particle-pitch angle scattering in the ICM can be provided by several processes discussed in the literature. Those include electron firehose instability which is indeed driven by pressure-anisotropies in high-beta plasma (Pilipp & Völk 1971; Paesold & Benz 1999), and gyroresonance by Alfvén (and slow) modes at small scales, provided that these modes are not too much anisotropic (cf. Yan & Lazarian 2004). The latter condition means that the Alfvénic modes are considered for scales not much less than $l_{\rm A}$, provided that the turbulence injection is isotropic. In addition, gyroresonance was discussed for the electrostatic lower hybrid modes generated by anomalous Doppler resonance instability due to pitch angle anisotropies (e.g. Liu & Mok 1977; Moghaddam-Taaheri et al. 1985) and by gyroresonant interaction with whistlers (e.g. Steinacker & Miller 1992). The latter process, however, is somewhat more problematic than the Alfvénic mode scattering, as whistler turbulence is even more anisotropic than the Alfvénic one (Cho & Lazarian 2004). Finally, instabilities within cosmic ray fluid look as a safer bet for isotropizing cosmic rays. For instance, Lazarian & Beresnyak (2006) proposed isotropization of cosmic rays due to gyroresonance instability that arises as the distribution of cosmic rays gets anisotropic in phase space. This instability that is customary discussed for plasma rather than for cosmic rays (see Gary et al. 1994) would guarantee that in the environments of galaxy clusters the TTD will not be quenched.

5.1.2 Diffusion coefficient

The momentum-diffusion coefficient, $D_{\rm pp}$, of particles can be calculated by deriving the first-order corrections due to small amplitude plasma turbulence to the orbits of particles in a uniform magnetic field, and ensemble averaging over the statistical properties of the turbulence (e.g. Jokipii 1966). The resulting analytic expressions for the pitch-angle and momentum-diffusion coefficients due to TTD resonance with fast modes in a low-beta plasma can be found in Schlickeiser & Miller (1998).

An additional and self-consistent way to derive the momentum-diffusion coefficient from the quasi-linear theory is to use an argument of detailed balancing. The diffusion coefficient of a α-species is indeed related to the damping rate of the modes themselves with the same particles, and one has (e.g. Eilek 1979; Achterberg 1981):

$$\int {\rm d}^3 p E_{\alpha} \left(\frac{\partial f_{\alpha}(p)}{\partial t}\right) = \int {\rm d}\boldsymbol{k} \Gamma^{\alpha}(k,\theta) \mathcal{W}(\boldsymbol{k}), \tag{35}$$

where E_{α} is the energy of a particle of species α, and $\mathcal{W}(\boldsymbol{k})$ is the total energy of the modes in the elemental range ${\rm d}\boldsymbol{k}$. This is given by

$$\mathcal{W}(\boldsymbol{k}) = \mathcal{W}_E(\boldsymbol{k}) \left(\frac{W}{W_E}\right)_{\boldsymbol{k}} = \frac{\mathcal{W}_E(k)}{4\pi k^2} \left(\frac{W}{W_E}\right)_{\boldsymbol{k}}, \tag{36}$$

where $(W/W_E)_{\boldsymbol{k}}$ is the ratio between the total and the electric energy in a single mode propagating at $\boldsymbol{k}$ (Section 4.2), and $\mathcal{W}_E(k)$ is the electric-field energy of the modes in the elemental range ${\rm d}k$. In equation (36) we have assumed an isotropic spectrum of the electric field fluctuations which is an appropriate assumption for super-Alfvénic turbulence and fast modes (e.g. CL03).

If isotropy of the particle momenta is *maintained*, the time evolution of the particle distribution function is related to the diffusion coefficient by

$$\frac{\partial f_\alpha(p)}{\partial t} = \frac{1}{p^2}\frac{\partial}{\partial p}\left(p^2 D_{\rm pp}\frac{\partial f_\alpha(p)}{\partial p}\right) \tag{37}$$

and thus equation (35) reads

$$\int {\rm d}^3 p \frac{E_\alpha}{p^2}\frac{\partial}{\partial p}\left[p^2 D_{\rm pp}\frac{\partial f_\alpha(p)}{\partial p}\right] = \frac{1}{2}\int {\rm d}k \int {\rm d}\theta \sin(\theta)\Gamma^\alpha(k,\theta)\mathcal{W}_E(k)\left(\frac{W}{W_E}\right)_{(\theta,k)}. \tag{38}$$

Here we are interested in deriving the diffusion coefficient in the case of relativistic species in the ICM (Sections 5.1.3 and 5.5). The damping with these particles (equation 31) can be expressed in the form

$$\Gamma^\alpha(k,\theta) = -\Gamma^\alpha(\theta)\, k \int p^4 {\rm d}p \frac{\partial f_\alpha(p)}{\partial p} \tag{39}$$

and from partial integration of equation (38) and from equations (39) and (31) taking $\mathcal{W}_{\rm B}(k) = (c/V_{\rm ph})^2\mathcal{W}_E(k)$, one gets

$$D_{\rm pp}(p) = \frac{\pi^2}{2}\frac{1}{c}p^2\frac{1}{B_{\rm o}^2}\int_0^{\pi/2}{\rm d}\theta V_{\rm ph}^2\frac{\sin^3(\theta)}{|\cos(\theta)|}\mathcal{H}\left(1-\frac{V_{\rm ph}/c}{\cos\theta}\right)\left[1-\left(\frac{V_{\rm ph}/c}{\cos\theta}\right)^2\right]^2\int {\rm d}k\mathcal{W}_{\rm B}(k)k. \tag{40}$$

This represents a self-consistent average (in terms of particle pitch-angle) momentum-diffusion coefficient of isotropic particles with momentum p which couple with fast magnetosonic modes via TTD resonance. Equation (40) in its low-beta plasma limit (essentially $V_{\rm ph} \rightarrow v_{\rm A}$ and $V_{\rm ph} \ll c$) is consistent with the expression (equation 29) given in Schlickeiser & Miller (1998) in its $z = k_\perp v_\perp/\Omega \ll 1$ limit and averaged over the particle pitch-angle.[10]

5.1.3 Acceleration efficiency in the ICM

As summarized in Section 3.5 we focus on a picture in which compressible turbulence is injected at large scales by the action of cluster mergers and accretion of matter. Provided that large-scale turbulence in the ICM is not significantly affected by the ion-viscosity (Section 3.4), an inertial range is established due to the combination of turbulence injection and cascading. For isotropic turbulence the diffusion equation in the k-space is given by

$$\frac{\partial\mathcal{W}(k,t)}{\partial t} = \frac{\partial}{\partial k}\left\{k^2 D_{kk}\frac{\partial}{\partial k}\left[\frac{\mathcal{W}(k,t)}{k^2}\right]\right\} - \sum_i \Gamma_i(k,t)\mathcal{W}(k,t) + I(k,t), \tag{41}$$

where D_{kk} is the diffusion coefficient in the k$-$*space*, $\Gamma_i(k,t)$ are the different damping terms (Section 4.3), and $I(k,t)$ accounts for the turbulence injection term. The wave–wave diffusion coefficient of magnetosonic modes (Kraichnan treatment; see also Zhou & Matthaeus 1990; Miller et al. 1996 for low-beta plasma) is given by[11]

$$D_{kk} \approx \langle V_{\rm ph}\rangle k^4\left[\frac{\mathcal{W}(k,t)}{\rho\langle V_{\rm ph}\rangle^2}\right]. \tag{42}$$

We assume a constant (in time) injection spectrum of the modes in the simple form $I(k) = I_{\rm o}\delta(k-k_{\rm o})$ so that the stationary spectrum of turbulence at the scales not significantly affected by dampings ($\Gamma_i \sim 0$) can be readily obtained from equation (41):

$$\mathcal{W}(k) = \left[\frac{2}{7}I_{\rm o}\rho\langle V_{\rm ph}\rangle\right]^{1/2}k^{-3/2} \tag{43}$$

and the cascading time at a the scale $l = 2\pi/k$, is given by

$$\tau_{kk} \approx \frac{k^3}{(\partial/\partial k)(k^2 D_{kk})} = \frac{2}{9}\left(\frac{7}{2}\frac{\langle V_{\rm ph}\rangle\rho}{I_{\rm o}}\right)^{1/2}k^{-1/2}. \tag{44}$$

Provided that the dissipation of compressible turbulence in the ICM is collisionless (Section 3.4), the turbulence cascading gets suppressed at a scale at which the resonant damping time-scale, Γ^{-1}, approach the cascading time. This scale is given by equation (44):

$$k_{\rm cut} \approx \frac{81}{14}\frac{I_{\rm o}}{\rho\langle V_{\rm ph}\rangle}\left[\frac{\langle\Gamma(k)\rangle}{k}\right]^{-2}, \tag{45}$$

where $\langle\Gamma\rangle$ is the average collisionless TTD-damping term given by equations (29), (31) and (33). The value of the cut-off scale is reported in Fig. 5(b) as a function of the beta of the plasma for physical conditions in the ICM (see caption): we find that if turbulence is energetic enough (actually for the values used in the Sections 5.3–5.5) compressible modes are dissipated at $\approx$ sub-kpc scales. The cut-off scale slightly increases in the case of small $\beta_{\rm pl}$ as the cascading of magnetosonic modes becomes less efficient (the cascading time-scale goes as $\tau_{kk} \propto$

[10] It is sufficient to integrate (average) equation (29) in Schlickeiser & Miller (1998) over the particle pitch-angle using the properties of the δ function, to solve this integration and to expand the Bessel function in equation (29) for small arguments.

[11] Here $\langle V_{\rm ph}\rangle$ is essentially a representative, averaged (with respect to θ) phase velocity.

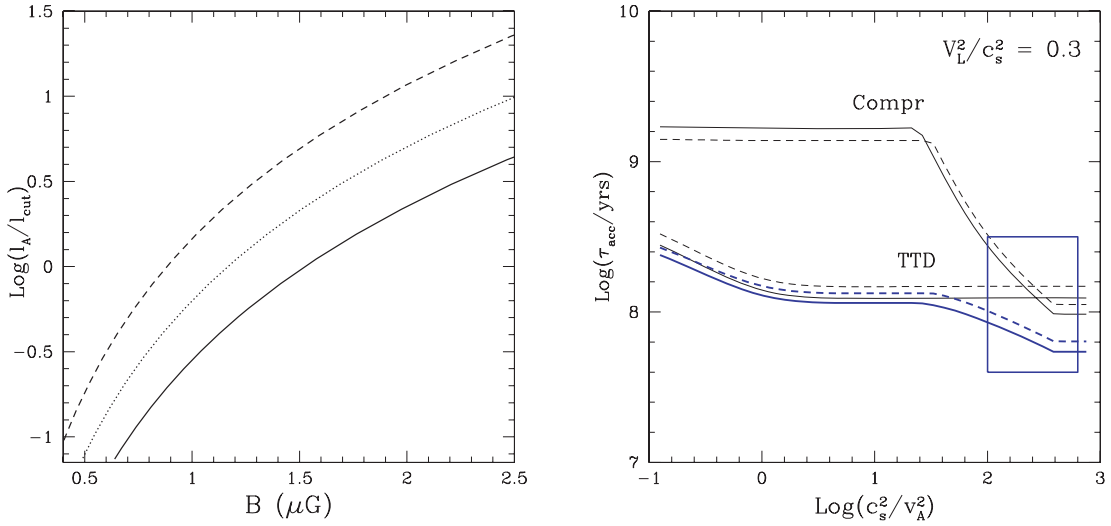

Figure 6. (a) The ratio l_A/l_{cut} is reported as a function of B. Calculations are reported for $k_B T = 6$ keV (dashed lines), 9 keV (dotted lines) and 12 keV (solid lines); $(V_L/c_s)^2 = 0.3, n_{th} = 10^{-3}$ cm^{-3} and $L_o = 300$ kpc were assumed in the calculations. (b) The acceleration time (equation 49) is reported as a function of c_s^2/v_A^2 in the case of non-resonant compressive acceleration (equation 51) and resonant TTD-acceleration (equation 47). Calculations are reported for $k_B T =$ 7 keV (dashed lines) and $k_B T = 11$ keV (solid lines); $(V_L/c_s)^2 = 0.3, n_{th} = 10^{-3}$ cm^{-3} and $L_o = 300$ kpc were assumed in the calculations. The acceleration time from the combined effect of the two mechanisms is also shown (ticked lines). The box marks the relevant range of the values of $c_s^2/v_A^2 (= \beta_{pl}/2)$ in the hot ICM, and the acceleration time necessary to boost relativistic electrons at several GeV (this accounts for both synchrotron and inverse Compton losses with redshift ∼0–0.3).

$\langle V_{ph} \rangle$ and, fixed c_s, increases for small β_{pl}). Actually the cascading of compressible motions is likely to reach MHD scales before being dissipated, $l_{cut} \leqslant l_A$ (Fig. 6a), and in this case it is also worth to mention that an Alfvénic turbulence can be activated by the cascading of these compressible motions.

Equation (41) is appropriate to describe the time evolution of the total spectrum of isotropic turbulent modes. On the other hand, formally in the collisionless regime the ratio between the energy of the fields (E and B) and that associated with particles changes with the mode-propagation angle (Figs 1 and 2, Appendix B). However, the induced anisotropy is within a factor of 2–3 for a stationary B_o, and it should be efficiently smoothed out by the effect of the bending of the field lines (Section 4.3). Thus we shall adopt isotropy as a viable approximation, and define the energy associated with the magnetic field fluctuations as

$$\mathcal{W}_B(k,t) \sim \frac{1}{\beta_{pl}} \left\langle \frac{\beta_{pl}|B_k|^2}{16\pi W(k)} \right\rangle \mathcal{W}(k,t), \tag{46}$$

where for consistency $|B_k|^2/W$ is taken from equation (24) and $\langle\rangle$ indicates the average over the propagation angle of the modes.

The TTD diffusion coefficient in the particle–momentum space is then obtained from equations (40), (43) and (46) in the form

$$D_{pp}(p,t) = \frac{\pi}{8} \frac{p^2}{c} \left\langle \frac{\beta_{pl}|B_k|^2}{16\pi W} \right\rangle \frac{1}{c_s^2} \left(\frac{2 I_o \langle V_{ph} \rangle}{7\rho} \right)^{1/2} k_{cut}(t)^{1/2} \int_0^{\pi/2} \mathrm{d}\theta V_{ph}^2 \frac{\sin^3(\theta)}{|\cos(\theta)|} \mathcal{H}\left(1 - \frac{V_{ph}/c}{\cos\theta}\right) \left[1 - \left(\frac{V_{ph}/c}{\cos\theta}\right)^2\right]^2. \tag{47}$$

Equation (47) allows a prompt estimate of the acceleration efficiency via TTD resonance, once the injection rate per unit mass of the compressible turbulence (I_o/ρ) and the injection scale, k_o (or L_o), are fixed:

$$\frac{I_o}{\rho} \approx \mathcal{C} V_L^3 k_o \left(\frac{V_L}{\langle V_{ph} \rangle} \right), \tag{48}$$

where $\mathcal{C} \approx 5$–6 is a numerical factor which can be readily obtained by taking $I_o/\rho \approx V_L^2/\tau_{LL}$ and equation (44). The resulting *systematic* acceleration rate, τ_{acc}, is given by

$$tau_{acc} = p^3 \left\{ \frac{\partial}{\partial p} \left[p^2 D_{pp}(p) \right] \right\}^{-1}. \tag{49}$$

The *systematic* acceleration time from TTD resonance does not depend on particle momentum (see also Fig. 7) and is reported in Fig. 6(b) as a function of $c_s^2/v_A^2 (= 2\beta_{pl})$: for a given temperature (and $\beta_{pl} > 1$) the acceleration efficiency scales approximately with $\sqrt{T}$ and is found to be almost independent from the value of β_{pl}. The important point here is that the strength of the TTD-acceleration efficiency, powered by compressible turbulence with large-scale rms velocity $V_L^2/c_s^2 \approx 0.3$, is found to give a *systematic* acceleration time of the order of $\sim 10^8$ yr which is sufficient to accelerate electrons up to energies of several GeV, and this may produce diffuse synchortron radio emission in μG-magnetized media (Section 6).

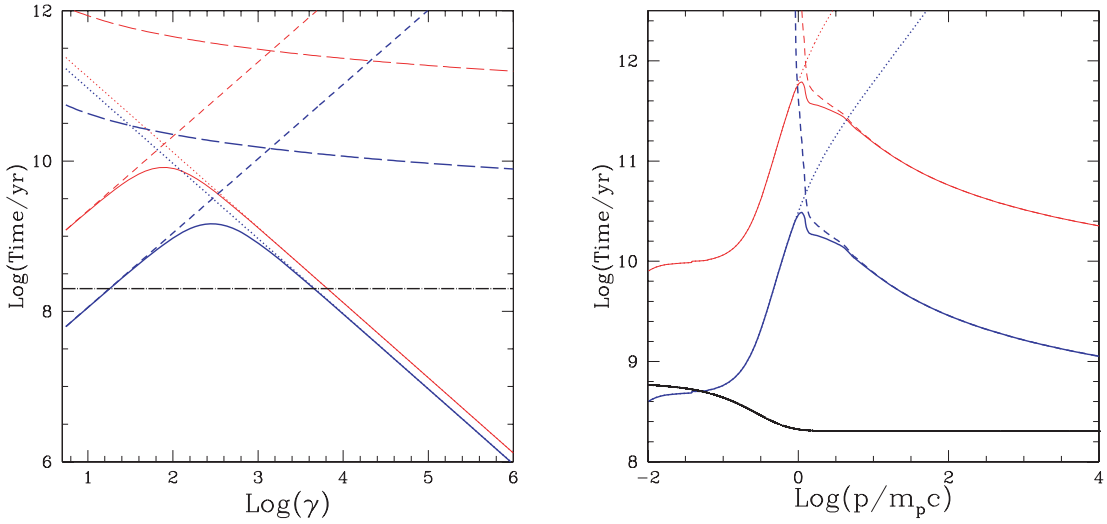

Figure 7. Left-hand panel: The lifetime of relativistic electrons in the ICM at $z = 0.2$ as a function of the Lorentz factor. Thick (blue) lines are for cluster cores and thin (red) lines are for cluster periphery. We report the total lifetime (solid lines) and the lifetimes due to single processes: Coulomb losses (dashed lines), synchrotron and IC losses (dotted lines) and bremsstrahlung losses (long dashed lines). Right-hand panel: The lifetime of cosmic ray protons in the ICM at $z = 0.2$ as a function of the particle momentum. Thick (blue) lines are for cluster cores and thin (red) lines are for cluster periphery. We report the total lifetime (solid lines) and the lifetimes due to single processes: Coulomb losses (dotted lines) and pp-collisions (dashed lines). In both panels calculations in the cores (thick blue) are obtained for $B = 3$ μG and $n_{\rm th} = 2 \times 10^{-3}$ cm^{-3}, and in the periphery (thin red) for $B = 0.5$ μG and $n_{\rm th} = 10^{-4}$ cm^{-3}. For comparison, the dash–dotted lines in both panels give the acceleration time-scale which is used in Fig. 8; note that the increase of this time-scale in the case of subrelativistic protons is due to the decrease of the efficiency of the non-resonant compression at subrelativistic energies.

5.2 Non-resonant acceleration

5.2.1 Introduction

Resonant TTD-acceleration is not the only process by which compressible turbulence may accelerate cosmic rays in the ICM. For instance, fast particles can be accelerated also by large-scale compressible motions (e.g. Ptuskin 1988; Chandran 2003; Chandran & Maron 2004; Cho & Lazarian 2006). Compression changes the particle momentum according to

$$\frac{\partial p}{\partial t} = -\frac{1}{3} p \ \nabla \cdot \boldsymbol{V}_l. \tag{50}$$

If the medium is neither expanding nor contracting it is $\langle \nabla \cdot \boldsymbol{V}_l \rangle = 0$ and thus particles will not experience regular changes in energy. On the other hand if $\boldsymbol{V}_l$ is a turbulent field a statistical acceleration effect (analogous to a classical second-order Fermi process) may exist. This is essentially because particles would statistically experience more compression than expansion.

5.2.2 Diffusion coefficient

Limiting to the case $V_l^2 \ll c_{\rm s}^2$ and provided that the turbulent velocity of the medium has correlation scales much longer than the effective particle mean free path, the diffusion coefficient in the particle momentum space, $D_{\rm pp}$, and the *total* (turbulent advection and diffusion) spatial diffusion coefficient, D_*, can be obtained by standard procedure in plasma physics in the quasi-linear approximation. These are (Ptuskin 1988)

$$D_{\rm pp} = \frac{2}{9} p^2 D \int_k \frac{{\rm d}y y^2 \mathcal{V}(y)}{c_{\rm s}^2 + y^2 D^2} \tag{51}$$

and

$$D_* = D \left[1 + \frac{4}{3} \int_k \frac{{\rm d}y \mathcal{V}(y)}{c_{\rm s}^2 + y^2 D^2} \right], \tag{52}$$

where D is the spatial particle-diffusion coefficient (without considering the effects induced by the non-resonant compressible coupling itself, equation 51), and $\mathcal{V}(y)$ is defined as

$$\int \mathcal{V}(y) \, {\rm d}y = V_{\rm L}^2. \tag{53}$$

In this regime slow and fast diffusion limit exist. In the slow limit the rate of particle diffusion out of compressible eddies is slower than the wave period, $\tau_{\rm w} \sim l/c_{\rm s}$, that is, $\tau_{\rm diff} \sim l^2/D \gg \tau_{\rm w}$ and $c_{\rm s}^2 \gg k^2 D^2$. Here the process is mainly contributed by the action of the smaller eddies in

the spectrum of the modes and it becomes faster as this minimum scale gets smaller (e.g. Cho & Lazarian 2006). From equation (51) we find

$$D_{\rm pp} \sim \frac{1}{9} p^2 \left(\frac{V_{\rm L}}{c_{\rm s}}\right)^2 D \left(\frac{1}{L_{\rm o} l^2}\right)^{2/3}_{l \sim l_{min}}. \quad (54)$$

For small minimum-turbulent scales this process formally becomes extremely efficient, however the minimum scale of the bulk of compressible turbulent eddies in the ICM cannot be very small as these modes are strongly damped (Section 5.1.3, Fig. 5).

In the opposite case, in the fast diffusion limit, particles leave the eddies before they turnover, that is, $\tau_{\rm diff} \ll \tau_{\rm w}$ and $c_{\rm s}^2 \ll k^2 D^2$. Here the process is mainly contributed by the action of the largest eddies which contain the bulk of the turbulent energy, and from equations (51) and (53) we find

$$D_{\rm pp} \sim \frac{2}{9} p^2 \frac{V_{\rm L}^2}{D}. \quad (55)$$

An important point discussed in Section 3.2 is that particle–spatial diffusion itself is likely to be affected by the turbulent bending of the magnetic field lines which gets the effective ion mean free path $\sim l_{\rm A}$. Compared to the Coulomb or gyroresonance scattering the diffusion with the characteristic scale $l_{\rm A}$ does not involve any changes of the particle energy via scattering. Therefore the particle may diffuse slowly, but the only change in energy will be due to large-scale compressions (cf. Cho & Lazarian 2006). We thus shall adopt a very simplified form of the spatial diffusion coefficient in equations (51)–(55):

$$D \sim \frac{c}{3} \beta \max\{l_{\rm cut},\ \min\{l_{\rm A},\ l_{\rm mfp}\}\}. \quad (56)$$

The combination between equations (51) and a turbulent-driven spatial diffusion coefficient (e.g. equation 56) provides an important refinement of the evaluation of the cosmic ray acceleration via compressible long wave turbulence, and may have important consequences in the case of the particle acceleration in the ICM (Section 5.3).

Finally, we want to remind that equation (51) is obtained by neglecting the effect of possible additional scattering processes due to resonant particle–wave interactions. The presence of instabilities in cosmic rays may create an additional slab-type Alfvénic component that would produce additional gyroresonance acceleration and reduce the effective mean free path (Lazarian & Beresnyak 2006). Conservatively we do not discuss this possibility in the present paper.

5.2.3 Acceleration efficiency in the ICM

In this section we calculate the efficiency of the particle acceleration from large-scale non-resonant compression in the ICM.

Taking a Kraichnan scaling for the super-Alfvénic compressible turbulence, $\mathcal{V}(k) \approx V_{\rm L}^2 k^{-3/2} / L_{\rm o}^{1/2}$, from equation (51) we have

$$D_{\rm pp} \simeq \frac{2}{9} D\, p^2 \frac{V_{\rm L}^2}{L_{\rm o}^{1/2}} \int_{1/L_{\rm o}}^{1/l_{\rm cut}} \frac{{\rm d}y\, y^{1/2}}{c_{\rm s}^2 + D^2 y^2}, \quad (57)$$

where the spatial-diffusion coefficient is given by equation (56).

The resulting *systematic* acceleration time is independent of particle momentum (at least in the ultrarelativistic case, see also Fig. 7) and is reported in Fig. 6(b). For a given temperature of the plasma, T, in the case of small $\beta_{\rm pl}$ the non-resonant compression is formally very inefficient because for large values of the magnetic field the particle spatial-diffusion coefficient is large (essentially $D \approx 1/3\, \beta c\, l_{\rm mfp}, l_{\rm mfp}$ from equation 1). On the other hand, in the case of large $\beta_{\rm pl}$ the acceleration efficiency increases because turbulence bends the magnetic field lines at scales smaller than $l_{\rm mfp}$ and the effective particle mean free path is $\approx l_{\rm A}$ (which scales as $\beta_{\rm pl}^{-3/2}$); saturation for large $\beta_{\rm pl}$ is reached when $l_{\rm cut} \geqslant l_{\rm A}$ (Fig. 6).

The reference value of $\beta_{\rm pl}$ in the ICM is in the range $\beta_{\rm pl} \sim$ 200–1000 (i.e. $B \sim$ 0.5–3 μG, with $n_{\rm th} \sim 10^{-4}$ to 10^{-3} cm^{-3} and $k_{\rm B} T \sim$ 7–10 keV), and formally under these conditions we find that the acceleration efficiency from non-resonant compression driven by relatively energetic turbulence (caption) is similar to that due to the TTD resonance.

As already pointed out in Section 5.2.2, in the derivation of equation (51) (or equation 57) it was assumed that the effective particle mean free path is much smaller than the scale of the turbulent eddies. This condition is formally violated in the case of small $\beta_{\rm pl}$ in Fig. 6(b) where the smaller turbulent eddies are $< l_{\rm mfp}$ (mean free path $l_{\rm mfp} \approx$ 10–50 kpc). On the other hand, this does not happen for larger $\beta_{\rm pl}$, since in this case the particle *effective* mean free path, $\approx l_{\rm A} \approx l_{\rm cut}$, is actually comparable to (or smaller than) the smallest turbulent eddies.

5.3 Overall effect of compressible turbulence

As discussed in Section 5.1.1 the TTD resonance is expected to be an efficient mechanism in the ICM, provided that particle isotropy is preserved. Yet the TTD alone might not be efficient enough in maintaining such isotropy because both $D_{\rm pp}(\mu, p)$ and $D_{\mu\mu}(\mu, p)$ are strongly maximized for particles moving at small angles with the direction of the seed magnetic field. However, additional resonant processes acting on small scales might easily maintain particle isotropy. If these mechanisms are really at work in the ICM they should also affect the spatial diffusion, D, of the particles and thus the efficiency of the non-resonant compression mechanism. Formally with decreasing D the non-resonant coupling with eddies in the fast diffusion limit becomes more efficient, and, at the same time, a larger range of scales of the eddies couples with particles in the slow diffusion regime which is very efficient; actually this is what happens with increasing the beta of the plasma in Fig. 6(b). However, if the spatial diffusion is strongly suppressed, namely, when $D < c_{\rm s} l_{\rm cut}$ in equations (51) and (57), one gets into the slow

diffusion limit at any turbulent scale, and a decrease of D yields a corresponding decrease in the efficiency of the non-resonant compression (equation 54). Thus future studies using self-consistent spatial diffusion coefficients will be of great importance.

The turbulent bending of the field lines which happens in the super-Alfvénic case cannot change the pitch angle of particles which would preserve the adiabatic invariant, however in the high-beta ICM turbulent bending is associated with turbulent compressions which indeed power the non-resonant acceleration mechanism and might provide a source of particle-pitch angle isotropization. The spatial diffusion coefficient is related to that in the pitch angle as (order of magnitude) $D \approx c^2/D_{\mu\mu}$, and the resulting time-scale of the pitch angle scattering, $\approx D_{\mu\mu}^{-1}$, is indeed much shorter than the acceleration time of fast particles (which is $\approx 10^7$–10^8 yr).

This is important since it implies that the action of large-scale compressible turbulence in the ICM is twofold. On one hand particles diffusing through the compressible turbulent eddies experience substantial non-resonant stochastic acceleration. On the other hand, even without requiring additional processes at small scales, this might contribute to help in maintaining particle–momentum isotropization, so that the compressive component of the turbulent magnetic field (that along $\boldsymbol{B}_o$) may also couple efficiently with particles via TTD resonance without greatly change the particle spatial diffusion.

These two mechanisms, TTD resonance and non-resonant compression, are driven by the same turbulent modes and involve independent particle-mode couplings and thus, as a first approximation, the acceleration process may be thought as the combination of the two effects; the deriving particle acceleration time is also reported in Fig. 6(b).

6 COMPRESSIVE TURBULENCE AND PARTICLE RE-ACCELERATION MODEL IN GALAXY CLUSTERS

As already anticipated in Section 1 direct evidence for relativistic electrons diffused on Mpc scales in the ICM comes from radio haloes and relics (e.g. Feretti 2005), while the hard X-ray tails detected in a few clusters may result from inverse Compton scattering of the cosmic microwave background photons by the same electrons (e.g. Fusco-Femiano et al. 2004; Rephaeli et al. 2006).

The particle re-acceleration model is a promising possibility to explain the properties of the giant radio haloes and possibly also the strength of the hard X-ray tails. This scenario assumes that turbulence is injected in a substantial fraction, Mpc^3, of the cluster volume during cluster–cluster mergers, and that relativistic electrons already present in the ICM and accumulated at $\gamma \approx 100$ are re-accelerated for a typical time-scale of $\leqslant$ Gyr (e.g. Brunetti et al. 2001; Petrosian 2001; Fujita, Takizawa & Sarazin 2003; Brunetti et al. 2004). Alternatively these seeds electrons to be re-accelerated could be secondary products of hadronic interactions (Brunetti & Blasi 2005).

In this section, after a brief review of the injection processes of cosmic rays in galaxy clusters and of the most relevant channels of energy losses (Section 6.1), we provide calculations in the context of the particle re-acceleration model which include the effect of TTD resonance and non-resonant acceleration due to compressible turbulent modes injected at large scales.

6.1 Cosmic ray injection in the ICM

There is a general consensus on the fact that several mechanisms of injection of cosmic rays may be at work in the ICM, and that once injected the bulk of these cosmic rays does not escape the cluster (e.g. Berezinsky, Blasi & Ptuskin 1997; Ensslin et al. 1998; Völk & Atoyan 1999).

Collisionless shocks are generally recognized as efficient particle accelerators through the so-called diffusive shock acceleration process (Drury 1983; Blandford & Eichler 1987). This mechanism has been invoked several times as an efficient acceleration process in clusters of galaxies (Takizawa & Naito 2000; Blasi 2001; Fujita & Sarazin 2001; Miniati et al. 2001; Ryu et al. 2003). Present simulations confirm the analytical claim that shocks with Mach number larger than 2–3 are rare (Gabici & Blasi 2003), and claim that the energy content in the form of cosmic rays in massive clusters may be of the order of a few per cent of the thermal energy (Jubelgas et al. 2006; Pfrommer et al. 2006). The bulk of the energy of these cosmic rays is injected in the cluster outskirts by shocks with a Mach number of the order of $\sim$3, the real efficiency of these shocks is however uncertain and it is generally computed according to the so-called *thermal leakage* model (e.g. Kang & Jones 2005).

A contribution to the injection of cosmic rays in clusters of galaxies may come from active galactic nuclei (AGNs) which indeed might fill the ICM with relativistic particles and magnetic fields, *extracted* from the accretion power of their central black hole (Ensslin et al. 1997). Similarly to AGNs, powerful Galactic winds may also inject relativistic particles and magnetic fields in the ICM (Völk & Atoyan 1999). Although the present-day level of starburst activity is low, it is expected that these winds were more powerful during starburst activity in early galaxies, as also suggested by the iron abundances in galaxy clusters (Völk, Aharonian & Breitschwerdt 1996).

6.2 Energy losses

6.2.1 Electrons and positrons

In the conditions typical of the ICM, ultrarelativistic electrons rapidly cool down through inverse Compton and synchrotron emission, and accumulate at Lorentz factors $\gamma \sim 100$–500 where they may survive for a few billion years before cooling further down in energy through Coulomb scattering and eventually thermalize. Energy losses and relevant time-scales of relativistic electrons in the ICM are discussed in several papers (e.g. Sarazin 1999; Petrosian 2001; Brunetti et al. 2004; Pfrommer & Ensslin 2004). In Fig. 7(a) we report the particle lifetime as a function of the Lorentz factor: the lifetime has a peak at $\gamma \approx 10^2$–10^3 where the cooling of electrons is slower and where particles

may accumulate providing a seed populations to be re-accelerated in the context of the re-acceleration model. More specifically, Fig. 7(a) is obtained for typical physical conditions in cluster cores and in the cluster outskirts: in the external regions of clusters electrons survive since Coulomb losses are less severe and in principle these particles can be accumulated for cosmological time-scales at energies $\gamma \sim 100$–1000. On the other hand, in cluster cores the higher thermal density limits the maximum lifetime of electrons at less than 1 Gyr.

6.2.2 Protons

Once injected the relativistic cosmic ray protons do not suffer catastrophic radiative-energy losses. The only relevant channel of energy losses for these particles in the ICM is given by hadronic collisions which however get a typical particle lifetime which is larger than a Hubble time for $\sim$ GeV particles. This, together with the long time necessary to the bulk of these cosmic rays to diffuse out of clusters, makes clusters themselves reservoir in which cosmic ray protons are confined and may accumulate over cosmological epochs (e.g. Völk et al. 1996; Berezinsky et al. 1997).

On the other hand, mildly and subrelativistic protons may be significantly affected by Coulomb energy losses, which in turn change the particle spectrum with respect to the injection spectrum. The rate of Coulomb losses is (e.g. Schlickeiser 2002)

$$\frac{\mathrm{d}p}{\mathrm{d}t}_{i}(\beta_{\rm p}) \approx -\frac{6}{\sqrt{\pi}} \times 10^{-29} n_{\rm th} \left\{ \int_0^{\beta_{\rm p}/\beta_{\rm e}} \mathrm{d}y \exp(-y^2) - \frac{\beta_{\rm p}}{\beta_{\rm e}} \left(1 + \frac{m_{\rm e}}{m_{\rm p}}\right) \exp\left[- \left(\frac{\beta_{\rm p}}{\beta_{\rm e}}\right)^2 \right] \right\}, \tag{58}$$

where $\beta_{\rm p}$ and $\beta_{\rm e} \sim 0.18\,(T/10^8\,K)^{1/2}$ are the velocity in units of the light speed of thermal electrons in the ICM and of the cosmic ray protons, respectively.

As in the case of leptons, the details of the mechanisms of energy losses of cosmic ray hadrons in the ICM can be found in several papers (e.g. Blasi & Colafrancesco 1999; Pfrommer & Ensslin 2004; Brunetti & Blasi 2005). In Fig. 7(b) we report the particle lifetime as a function of the particle momentum. Fig. 7(b) is obtained for typical physical conditions in cluster cores and in the cluster outskirts: it is clear that even in the cluster cores where losses are much severe the bulk of relativistic protons has a lifetime of the order of a Hubble time. Only protons with kinetic energy larger than about 200 GeV and smaller than about 30 MeV in the cluster cores have lifetimes smaller than a couple of Gyr, while just out of the core regions the lifetime of these particles grows (time $\propto n_{\rm th}^{-1}$) and all these particles are expected to survive for cosmological time-scales.

6.3 Numerical calculations

In this section we calculate the time evolution of the spectrum of the relativistic particles stochastically re-accelerated by turbulent modes in the ICM.

6.3.1 Formalism

As discussed in Section 5 we shall assume isotropy of the particle momenta and of the modes, and in this case the time evolution of the spectrum of the turbulent modes and of the particles can be formally derived by a set of coupled kinetic equations. The time evolution of the spectrum of the leptonic component is given by

$$\frac{\partial N_{\pm}(p,t)}{\partial t} = \frac{\partial}{\partial p}\left[N_{\pm}(p,t) \left(\frac{\mathrm{d}p}{\mathrm{d}t}_{\rm rad} + \frac{\mathrm{d}p}{\mathrm{d}t}_{\rm i} - \frac{2}{p}\left\{ D^r_{\rm pp} + D^c_{\rm pp} \right\} \right) \right] + \frac{\partial}{\partial p}\left[\left\{ D^r_{\rm pp} + D^c_{\rm pp} \right\} \frac{\partial N_{\pm}(p,t)}{\partial p} \right] + Q_{e^{\pm}}(N_{\rm p}(p,t); p, t), \tag{59}$$

where N_- and N_+ stands for electrons and positrons ($N = 4\pi p^2 f, f$ is used in Section 4), respectively, and where the terms $\mathrm{d}p/\mathrm{d}t_{\rm rad}$ and $\mathrm{d}p/\mathrm{d}t_i$ account for radiative (synchrotron and IC) and Coulomb losses, while $D^r_{\rm pp}$ and $D^c_{\rm pp}$ are the resonant (TTD, equation 47) and the non-resonant (from turbulent-compression, equation 57) particle momentum-diffusion coefficients. In equation (59) we also formally include an injection term, $Q_{e^{\pm}}(N_{\rm p}(p,t); p, t)$, which depends on the spectrum of cosmic ray protons, and is necessary in the case that the re-accelerated electrons and positrons are injected by hadronic collisions in the ICM (see Brunetti & Blasi 2005).

The time evolution of the spectrum of cosmic ray protons is given by

$$\frac{\partial N_{\rm p}(p,t)}{\partial t} = \frac{\partial}{\partial p}\left[N_{\rm p}(p,t) \left(\frac{\mathrm{d}p}{\mathrm{d}t}_{\rm i} - \frac{2}{p}\left\{ D^r_{\rm pp} + D^c_{\rm pp} \right\} \right) \right] + \frac{\partial}{\partial p}\left[\left\{ D^r_{\rm pp} + D^c_{\rm pp} \right\} \frac{\partial N_{\rm p}(p,t)}{\partial p} \right], \tag{60}$$

where the term $\mathrm{d}p/\mathrm{d}t_i$ accounts for Coulomb losses (equation 58), while the particle depletion due to proton–proton collisions can be neglected. Because the population of cosmic ray protons in the ICM essentially comes from the accumulation of these particles during cosmological time-scales, we do not consider the source term in equation (60) which would account for the contribution from freshly injected protons.

The evolution of the spectrum of the compressible turbulent modes is given by equation (41) described in Section 5.1.3, where all the dampings are formally derived in combination with equations (59) and (60). The effect of the non-resonant damping on the spectrum of the modes can be neglected since turbulent-compression acts efficiently only on relativistic particles in the ICM (Section 5.2), and this gets a net damping rate which is much smaller than that via TTD resonance with the thermal ICM.

6.3.2 Assumptions

In this paper we adopt the particle re-acceleration model assuming that a seed population of relativistic electrons and protons in the ICM is re-accelerated by turbulence injected at large scales during a merger event. For simplicity we do not study the more complex issue of the re-acceleration of secondary electrons and positrons injected by proton collisions in the ICM (Brunetti & Blasi 2005).

The *originality of this paper* is that compressible turbulence is used as the driving of particle re-acceleration, and accordingly the detailed diffusion coefficients obtained in Section 5 and the scenario and properties of turbulence discussed in Sections 3 and 4 are used in the calculations. For seek of clarity the main assumptions and physical parameters used in the calculations are listed below.

(i) We consider physical parameters appropriate for massive galaxy clusters: $T \approx 10^8$ K, $n_{\rm th} \approx 10^{-3}\,{\rm cm}^{-3}$, $B \approx 0.5$–3 μG.

(ii) Turbulence is assumed to be subsonic, with $V_{\rm L}^2 \ll c_{\rm s}^2$, and injected at large scales $L_0 \approx$ 300–500 kpc for a typical cluster–cluster crossing time.

(iii) The initial spectrum of electrons, $N_{\rm e}(p, t = 0)$, is derived by assuming that electrons are injected in the ICM in a single event and then evolve passively for ≈1–3 Gyr before being re-accelerated (see Brunetti et al. 2004).

(iv) The initial spectrum of protons, $N_{\rm p}(p, t = 0)$, is derived by assuming that protons are continuously injected in the ICM for a long period, ≈3–5 Gyr, with a constant injection spectral rate $Q \propto p^{-2.2}$ before being re-accelerated (see Brunetti et al. 2004).

(v) Damping terms from relativistic species in equation (41) are neglected in the calculations as they become important only if the relativistic component gets a relevant fraction of the thermal energy of the ICM (Section 4.3).

(vi) The damping term due to thermal particles is taken stationary because, under the assumption (ii), the thermal properties of the ICM are not significantly modified with time.

Under conditions (ii), (v) and (vi) the spectrum of the modes is also stationary and this is given by equation (43).

6.3.3 Main results

Once large-scale turbulence is injected in the ICM, magnetosonic modes take a relatively long time to cascade at collisionless scales:

$$\tau_{kk}\,({\rm Gyr}) \approx 0.6 \left(\frac{L_{\rm o}}{300\ {\rm kpc}}\right) \left(\frac{V_{\rm L}}{10^3\ {\rm km\,s^{-1}}}\right)^{-1} \left(\frac{M_{\rm s}}{0.5}\right)^{-1}. \quad (61)$$

In the re-acceleration scenario this is an unavoidable temporal gap, of a fraction of a Gyr, between the injection of the first turbulent eddies and the beginning of the particle re-acceleration process. When turbulence reaches collisionless scales the acceleration process starts and particles take a time, of the order of the re-acceleration time, to be significantly boosted in energy. A relevant example of the time evolution of the electron and proton spectrum during the re-acceleration period is reported in Fig. 8 assuming $V_{\rm L}^2 \sim 0.18\, c_{\rm s}^2$ (see caption): the seed electrons initially accumulated at $\gamma \sim 10^2$–10^3 are efficiently re-accelerated up to $\gamma \approx 10^4$–10^5.

Radio (and hard X-rays) observations can be well explained in terms of a high-energy *tail* of emitting relativistic electrons at energies of several GeV (e.g. Schlickeiser et al. 1987; Brunetti et al. 2001; Petrosian 2001). We calculate the evolution of the re-accelerated particles under the conditions given in Section 6.3.2 and find that, quite independently from the initial electron and proton spectrum, an appreciable

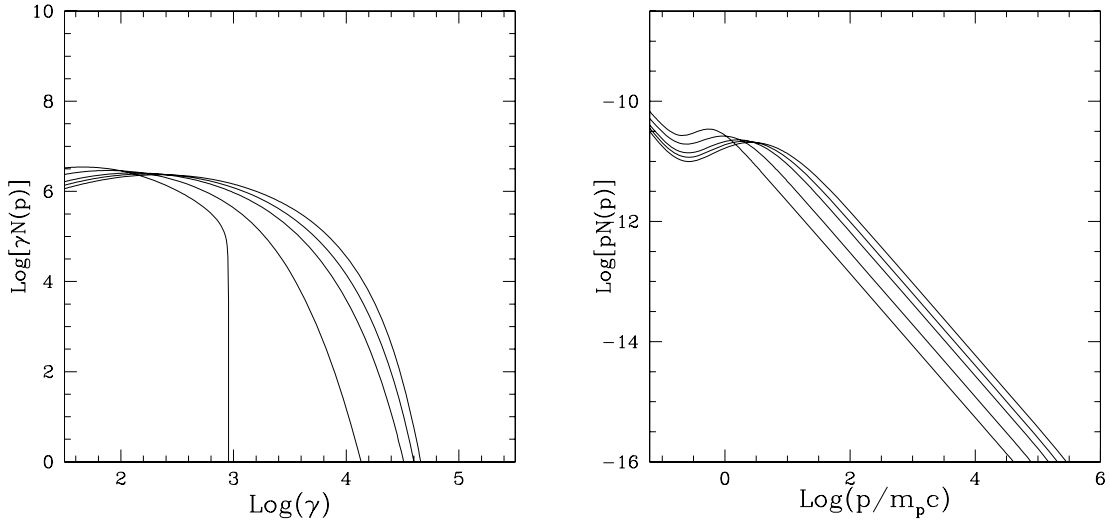

Figure 8. Left-hand panel: Time evolution of the spectrum of relativistic electrons as a function of the Lorentz factor. Right-hand panel: Time evolution of the spectrum of cosmic ray protons as a function of the particle momentum. In both panels calculations are reported for: $t = 0, 4 \times 10^{15}, 8 \times 10^{15}, 10^{16}, 1.2 \times 10^{16}$ s from the start of the re-acceleration phase. Calculations are performed assuming $(V_{\rm L}/c_{\rm s})^2 = 0.18$, $L_{\rm o} = 300$ kpc, $n_{\rm th} = 10^{-3}$, $k_{\rm B}T = 9$ keV, $B = 1$ μG and redshift $z = 0.1$ (for IC losses).

high-energy tail of relativistic electrons at these energies is produced approximately for $(V_L/c_s)^2 \geqslant 0.15\,(1+z/0.1)^2$.[12] In this case compressible turbulence injected at large scales in galaxy clusters may actually trigger efficient particle re-acceleration, and potentially explain the diffuse Mpc radio sources observed in massive galaxy clusters and the hard X-rays in excess to the thermal X-ray emission.

A spectral break, at $\approx$ GHz frequencies, is observed in the synchrotron spectrum of a few radio haloes and this is interpreted in favour of the re-acceleration scenario (e.g. Brunetti 2004; Feretti 2005). Under the condition (i) in Section 6.3.2, such a break requires the presence of a corresponding break in the spectrum of the emitting electrons at energies $\approx$5–10 GeV, and we find that this is reproduced by our re-acceleration model in the case of *moderate* turbulence, typically $(V_L/c_s)^2 \sim 0.15$–0.25, while in the case of more energetic turbulence electrons can be re-accelerated at larger energies and the corresponding synchrotron break is shifted at several GHz.

Also protons are efficiently re-accelerated. Relativistic protons are not subject to radiative losses and since the re-acceleration efficiency scales with the energy of the particles (Sections 5.1 and 5.2) the spectrum is simply shifted at higher energies and the slope of the injection spectrum is essentially preserved during the re-acceleration (Fig. 8).

Under our assumption (v), Section 6.3.2), it is $\Gamma_{th} \gg \Gamma_{rel}$ and the spectrum of the turbulent fluctuations in terms of magnetic field, $\mathcal{W}_B$, does not depend on the presence of cosmic rays, thus protons cannot significantly affect the acceleration process of relativistic electrons. This marks an important difference with Alfvénic re-acceleration, in which case the dominant damping of the modes comes from the resonance with relativistic protons and thus these protons affect the electron acceleration (*Wave–proton Boiler*, Brunetti et al. 2004).

An additional point to stress here is that, because $\Gamma_{th} \gg \Gamma_{rel}$, the fraction of the turbulent energy which goes into the cosmic rays via TTD resonance is simply $\approx \Gamma_{rel}/\Gamma_{th}$ and is fixed by the fraction of the energy in the ICM which is in the form of cosmic rays. An additional contribution to the energy of the re-accelerated particles comes from the non-resonant compression. In our calculations (assuming that cosmic rays store a few per cent of the thermal energy in the ICM) the total fraction of the turbulent energy which goes into non-thermal particles is of the order of $\approx$2–5 per cent.

In case of long re-acceleration periods, actually $\geqslant$3–4 times the re-acceleration time (equation 49), a non negligible fraction of the electron number is boosted towards the maximum energy. Here an equilibrium between acceleration and losses is reached and most of the energy flux from the damping of the turbulence with these particles is radiated away via synchrotron and IC by the same re-accelerated particles. Thus in principle for very long re-acceleration periods the total energy of the electron population should saturate and the spectrum is expected to slowly approach stationary conditions. On the other hand, since cosmic ray protons are free from energy losses, the energy flux from the damping of the turbulence is totally stored in the form of particle energy and this gives an *unbalance* between electron and proton acceleration. In the re-acceleration scenario this *unbalance* is not expected to be large, indeed turbulence is injected during cluster mergers and the duration of a re-acceleration period is constrained by the cluster–cluster crossing time and by the turbulence cascading time, and these cannot significantly exceed about 1 Gyr (see equation 61). In addition, present studies of the number counts of giant radio haloes in galaxy clusters limit the lifetime of these sources at about $\approx$1 Gyr (e.g. Hwang 2004) and this additionally constraints the duration of stochastic particle re-acceleration periods in galaxy clusters. Actually, given these limits, we find that assuming $(V_L/c_s)^2 \sim 0.15$–0.25 (which is required to provide the necessary electron re-acceleration up to $\approx$5–10 GeV) and a duration of the re-acceleration *phase* in the range 0.4–1 Gyr, the total energy of the cosmic ray protons and that of the relativistic electrons are both boosted by a factor of 1.5–4, and the *unbalance* is not substantial.

7 DISCUSSION

7.1 Major results

The problem of proton and electron stochastic re-acceleration by compressible motions is a complex one. The efficiency of acceleration depends on the spectrum of compressible turbulent motions. The extent and the shape of this spectrum, in its turn depend on the processes of plasma damping. In the case of the hot ICM the corresponding issues have not yet been clarified sufficiently in the literature.

As a result, we had to address those issues one by one. Namely, we started with the problem of describing turbulence in ICM in Section 3. First of all, we provided arguments suggesting that turbulence is expected to be present in the medium in hot (and massive) galaxy clusters. This is also because the ICM is magnetized and this implies a partial suppression of the plasma viscosity. The suppression of the viscosity in a magnetized medium is a well-known effect and has been addressed at least for laminar flows (e.g. Simon 1955). In the case of the strongly super-Alfvénic turbulence in the ICM an additional effect comes due to the bending of the field lines. Field lines are bended on scales $< l_{mfp}$ and this affects the ion diffusion process and thus viscosity. An additional suppression of the viscosity might come from the effect of plasma instabilities which affect the ion–ion mean free path, but that are not considered in this paper. Then, as we are interested in the compressible motions we discussed their generation in super-Alfvénic and MHD turbulence along with providing the estimates for collisional and collisionless damping of such motions. The outcome of Section 3 is a validation of a basic features of scenario according to which the energy can be injected due to cluster mergers on large scales and energize the particles in the ICM.

The quantitative treatment of the particle re-acceleration requires a much more rigorous treatment of mode spectrum and damping which was non trivial. In Section 4 we make use of collisionless physics and quasi-linear theory and derive general formulae for the spectrum of the compressible modes, basically the ratio between the energy in magnetic fluctuations and the total energy in the mode, and for the damping rate in magnetized plasma, and re-obtained expressions known in the literature, as a particular cases of our approach. The importance of the

[12] The term $(1+z/0.1)$ comes from IC losses (as for $B \approx \mu$G synchrotron losses are subdominant).

derived formulae goes beyond our particular case of study, as a rigorous description of damping is important for many other astrophysical important situations, for example, in galactic environments (see Yan & Lazarian 2004).

Having at hand a description of compressible super-Alfvénic and MHD turbulence with specified injection and damping scales we studied in Section 5 proton and electron stochastic re-acceleration by compressible modes. We focus on particle acceleration from magnetosonic modes and neglect the contribution from slow modes and Alfvén modes. Slow modes are subdominant for particle re-acceleration as they have a phase velocity $\ll$ than that of fast modes and sound waves, in addition both slow modes and Alfvén modes get anisotropic at small scales (if injected at large scales) and this reduces the efficiency of gyroresonance acceleration. We showed that because of efficient damping of fast modes at small scales the acceleration by gyroresonance is suppressed, that is, only extremely high-energy protons with large gyroradius can find magnetic perturbations to resonate with. Thus we study stochastic re-acceleration by both non-resonant large-scale compressions and resonant TTD, and clarified the regimes when the non-resonant large-scale compressions is important. The acceleration picture that is drawn from this paper is complex. In the case of super-Alfvénic turbulence in the ICM the turbulent bending of magnetic field lines limits particle spatial diffusion. Because line bending is associated with turbulent compression fast particles diffusing through the compressible turbulent eddies may experience efficient stochastic acceleration via *Fermi II* non-resonant-turbulent compression. The same particles can also experience coupling with these compressible eddies via TTD resonance which is found to be efficient in the ICM provided that particle pitch-angle isotropization is maintained.

Finally, in Section 7, we apply our results to the case of the particle re-acceleration scenario which is proposed to explain radio haloes (and hard X-ray tails) in galaxy clusters. Our calculations showed that the acceleration of energetic particles in galaxy clusters may be efficient. Relativistic electrons in the ICM can be re-accelerated against radiative and Coulomb losses up to energies of several GeV (or more) assuming that compressible turbulence at large scales stores a *non-negligible* fraction of the thermal energy, namely, $(V_{\rm L}/c_{\rm s})^2 \geqslant 0.15$. These electrons would emit Mpc-scale synchrotron radiation up to GHz frequencies (or more) provided that the magnetic field in the ICM is at $\approx \mu$G level on these scales. In addition, it also comes out that the re-acceleration of these electrons happens without transferring too much energy to protons, which might alleviate possible problems of earlier re-acceleration models that appealed to Alfvén modes.

7.2 Simplifying assumptions

In other words, the proposed re-acceleration scenario, which makes use of compressible modes, is a plausible one and deserves further studies. At the moment it includes several simplifications. In particular, plasma instabilities can decrease further mean free path of protons, which would decrease damping of turbulence. As a result, compressible modes could cascade to smaller scales, making, for instance, gyroresonance acceleration by fast modes more efficient. An effect related to the gyrokinetic instability in accelerated particles (Lazarian & Beresnyak 2006) may act in a different direction suppressing compressible motions at small scales, however on the other hand the Alfvénic component generated by this instability may also accelerate particles. Plasma instabilities might also affect the diffusion of fast particles and this might be important in the calculation of the efficiency of the acceleration from non-resonant compression.

In addition, reconnection processes taking place in the magnetized plasma should be able to accelerate particles on their own. Within small volume current sheets, the percentage of accelerated particles is small. However, stochastic reconnection model in Lazarian & Vishniac (1999) allows acceleration of a substantial part of particles at the expense of the magnetic energy in the turbulent plasmas (De Gouveia dal Pino & Lazarian 2005). Therefore we believe that our treatment would underestimate the actual acceleration; further research should clarify the actual picture.

Our derivations of the damping rates are valid when the ratio of the imaginary to the real part of the mode-frequency is much less than unity. This is generally true in the ICM and is a natural assumption for dealing with turbulence cascade, as in the opposite regime, no cascading is possible and the energy dissipates at the injection scale.

7.3 Relation to earlier works

Stochastic particle acceleration in galaxy clusters has been addressed by several papers (e.g. Schlickeiser et al. 1987; Brunetti et al. 2001; Petrosian 2001; Fujita et al. 2003). This work appeals to compressible motions to re-accelerate particles in the ICM. Earlier detailed time-dependent calculations of the problem of re-acceleration was addressed in Brunetti et al. (2004) and Brunetti & Blasi (2005), where Alfvén modes were used for the purpose. Such an approach is adequate if, for instance, Alfvén modes are injected by some mechanism at small scales. One possibility is that this might happen in the gyrokinetic instability scenario (Lazarian & Beresnyak 2006), and this provides an interesting possibility that we consider elsewhere. If, however, Alfvén modes are injected at large scales the Alfvénic component at the scale of energetic particle gyroradius gets very anisotropic and interacts very inefficiently with the particles (Chandran 2000; Yan & Lazarian 2002). Thus fast compressible modes should be considered. These modes are isotropic and may scatter particles efficiently as we have demonstrated above.

In some aspects the scenario suggested in the present paper for the ICM is similar to that adopted to calculate the *scattering* of galactic cosmic rays in Yan & Lazarian (2004), and to that adopted in the ICM by Cassano & Brunetti (2005).

The present paper is a *theoretical extension* of the work of Cassano & Brunetti (2005) where a more simplified treatment of the resonant TTD re-acceleration of electrons by fast modes was used to derive the statistical properties of non-thermal emission in galaxy clusters.

Yan & Lazarian (2004) discuss cosmic rays propagation in Milky Way thus focusing on MHD turbulence at scales $l < l_{\rm A}$ and mostly low-beta plasma. On the other hand, here we concentrated on the acceleration by motions at scales larger than $l_{\rm A}$ and high-beta plasma, the

conditions which are relevant to the clusters of galaxies. This made our calculations of the particle-mode damping rates and of the particle-diffusion coefficients different from those in Yan & Lazarian (2004). In particular, we had to re-adopt many of the plasma results for high-beta plasma and to treat differently magnetic field wandering.

Finally, an additional new of this paper is that we not only considered acceleration of electrons by the TTD resonance, but acceleration of fast protons and electrons subjected to both the TTD resonance and the large-scale compressions.

8 SHORT SUMMARY

The paper above explains the non-thermal emission observed in galaxy clusters as a consequence of electron re-acceleration by compressible turbulence. In this scenario turbulence is injected at the scale of galaxy mergers and cascades to small scales where the bulk of energetic particle acceleration happens. The turbulence is described by using the recent advances in understanding of MHD turbulence. The paper incorporates the following.

(I) A model of compressible turbulence in galaxy clusters. In this model the energy is injected at the scale of galaxy mergers and cascades to small scales where the bulk of energetic particle acceleration happens.

(II) Calculations of the plasma damping and energy of the mode for an arbitrary angle of wave propagation to magnetic field and a rather general model of plasma.

(III) Calculations of acceleration of protons and electrons by compressible motions in ICM plasma and a detailed application to the particle re-acceleration scenario to explain radio haloes and possibly hard X-ray tails.

Our results show that electrons obtain a substantial part of the energy transferred to the energetic particles, which fits well to the existing observational constraints.

ACKNOWLEDGMENTS

We thank the referee V. Petrosian for very useful comments and discussions, and R. Cassano and V. Dogiel for comments on the manuscript. We acknowledge partial support from MIUR through grant Cofin2004. GB thanks partial support from MIUR through grant PRIN2005. AL acknowledges NASA NNG05GGF57G and the NSF Centre for Magnetic Self-Organization in Laboratory and Astrophysical Plasmas.

REFERENCES

Achterberg A., 1981, A&A, 97, 259
Akhiezer A. I., Akhiezer I. A., Polovin R. V., Sitenko A. G., Stepanov K. N., 1975, Plasma Electrodynamics. Pergamon, Oxford
Barnes A., 1968, Phys. Fluids, 11, 2644
Barnes A., Scargle J. D., 1973, ApJ, 184, 251 (BS73)
Baldwin D. E., Bernstein I. B., Weenink M. P. H., 1969, Adv. Plasma Phys., 3, 1
Becker P. A., Le T., Dermer C. D., 2006, ApJ, 647, 539
Berezinsky V. S., Blasi P., Ptuskin V. S., 1997, ApJ, 487, 529
Bertoglio J. P., Bataille F., Marion J. D., 2001, Phys. Fluids, 13, 290
Blandford R., Eichler D., 1987, Phys. Rep., 154, 1B
Blasi P., 2001, Astropart. Phys., 15, 223
Blasi P., 2004, JKAS, 37, 483
Blasi P., Colafrancesco S., 1999, Astropart. Phys., 12, 169
Blasi P., Gabici S., Brunetti G., 2007, Int. J. Mod. Phys. A, 22, 681
Braginskii S. I., 1965, Rev. Plasma Phys., 1, 205
Brunetti G., 2003, in Bowyer S., Hwang C.-Y., eds, ASP Conf. Ser. Vol. 301, Matter and Energy in Clusters of Galaxies. Astron. Soc. Pac., San Francisco, p. 349
Brunetti G., 2004, JKAS, 37, 493
Brunetti G., 2006, Astron. Nachr., 327, 615
Brunetti G., Blasi P., 2005, MNRAS, 363, 1173
Brunetti G., Setti G., Feretti L., Giovannini G., 2001, MNRAS, 320, 365
Brunetti G., Blasi P., Cassano R., Gabici S., 2004, MNRAS, 350, 1174
Buote D. A., 2001, ApJ, 553, L15
Cassano R., Brunetti G., 2005, MNRAS, 357, 1313
Chandran B. D. G., 2000, Phys. Rev. Lett., 85, 4656
Chandran B. D. G., 2003, ApJ, 599, 1426
Chandran B. D. G., Maron J. L., 2004, ApJ, 603, 23
Cho J., Lazarian A., 2002, ApJ, 575, L63
Cho J., Lazarian A., 2003, MNRAS, 345, 325 (CL03)
Cho J., Lazarian A., 2004, ApJ, 615, L41
Cho J., Lazarian A., 2006, ApJ, 638, 811
Cho J., Lazarian A., Vishniac E. T., 2002, ApJ, 564, 291
Cho J., Lazarian A., Honein A., Knaepen B., Kassinos S., Moin P., 2003, ApJ, 589, L77
Churazov E., Forman W., Jones C., Sunyaev R., Böhringer H., 2004, MNRAS, 347, 29
Crawford C. S., Hatch N. A., Fabian A. C., Sanders J. S., 2005, MNRAS, 363, 216

De Gouveia dal Pino E. M., Lazarian A., 2005, A&A, 441, 845
Denisse J. F., Delcroix J. L., 1963, Plasma Waves. Interscience, New York
Dennison B., 1980, ApJ, 239, L93
Dogiel V. A., Colafrancesco S., Ko C. M., Kuo P. H., Hwang C. Y., Ip W. H., Birkinshaw M., Prokhorov D. A., 2007, A&A, 461, 433
Dolag K., Bartelmann M., Lesch H., 2002, A&A, 387, 383
Dolag K., Vazza F., Brunetti G., Tormen G., 2005, MNRAS, 364, 753
Drury L., 1983, Space Sci. Rev., 36, 57
Eilek J. A., 1979, ApJ, 230, 373
Eilek J. A., Henriksen R. N., 1984, ApJ, 277, 820
Ensslin T. A., Biermann P. L., Kronberg P. P., Wu X.-P., 1997, ApJ, 477, 560
Ensslin T. A., Wang Y., Nath B. B., Biermann P. L., 1998, A&A, 333, L47
Ensslin T. A., Vogt C., Pfrommer C., 2005, in Chyzy K. T., Otminowska-Mazur K., Soida M., Derrmar R.-J., eds, The Magnetized Plasma in Galaxy Evolution. Jagielonian University, Kracow, p. 231
Fabian A. C., Sanders J. S., Crawford C. S., Conselice C. J., Gallagher J. S., Wyse R. F. G., 2003, MNRAS, 344, L48
Farmer A. J., Goldreich P., 2004, ApJ, 604, 671
Feretti L., 2005, Adv. Space Res., 36, 729
Fermi E., 1949, Phys. Rev., 75, 1169
Fisk L. A., 1976, J. Geophys. Res., 81, 4633
Foote E. A., Kulsrud R. M., 1979, ApJ, 233, 302
Fried B. D., Conte S. D., 1961, The Plasma Dispersion Function. Academic Press, New York
Fujita Y., Sarazin C. L., 2001, ApJ, 563, 660
Fujita Y., Takizawa M., Sarazin C. L., 2003, ApJ, 584, 190
Fujita Y., Matsumoto T., Wada K., 2004, ApJ, 612, L9
Fusco-Femiano R., Orlandini M., Brunetti G., Feretti L., Giovannini G., Grandi P., Setti G., 2004, ApJ, 602, L73
Gabici S., Blasi P., 2003, ApJ, 583, 695
Gary S. P., McKean M. E., Winske D., Anderson B. J., Denton R. E., Fuselier S. A., 1994, J. Geophys. Res., 99, 5903
Gastaldello F., Molendi S., 2004, ApJ, 600, 670
Ginzburg V. L., 1961, Propagation of Electromagnetic Waves in Plasma. Gordon & Breach, New York
Goldreich P., Sridhar S., 1995, ApJ, 438, 763 (GS95)
Govoni F., Feretti L., 2004, Int. J. Mod. Phys., 13, 1549
Higdon J. C., 1984, ApJ, 285, 109
Hwang C-Y., 2004, JKAS, 37, 461
Jaffe W. J., 1977, ApJ, 212, 1
Jokipii J. R., 1966, ApJ, 146, 480
Jubelgas M., Springel V., Ensslin T. A., Pfrommer C., 2006, A&A, submitted (astro-ph/0603485)
Kang H., Jones T. W., 2005, ApJ, 620, 44
Kato S., 1968, PASJ, 20, 59
Kowal G., Lazarian A., 2006, preprint (astro-ph/0611396)
Krall N. A., Trivelpiece A. N., 1973, Principles of Plasma Physics. McGraw-Hill, New York
Lazarian A., 2006a, Astron. Nachr., 327, 609
Lazarian A., 2006b, ApJ, 645, L25
Lazarian A., Beresnyak A., 2006, MNRAS, 373, 1195
Lazarian A., Vishniac E. T., 1999, ApJ, 517, 700
Lithwick Y., Goldreich P., 2001, ApJ, 562, 279
Liu C. S., Mok Y., 1977, Phys. Rev. Lett., 38, 162
Melrose D. B., 1968, Ap&SS, 2, 171
Miller J. A., 1991, ApJ, 376, 342
Miller J. A., La Rosa T. N., Moore R. L., 1996, ApJ, 461, 445
Miniati F., Jones T. W., Kang H., Ryu D., 2001, ApJ, 562, 233
Moghaddam-Taaheri E., Vlahos L., Rowland H. L., Papadopoulos K., 1985, Phys. Fluids, 28, 3356
Montgomery D., Brown M. R., Matthaeus W. H., 1987, J. Geophys. Res., 92, 282
Narayan R., Medvedev M. V., 2001, ApJ, 562, L129
Paesold G., Benz A. O., 1999, A&A, 351, 741
Percival D. J., Robinson P. A., 1998, J. Math. Phys., 39, 3678
Petrosian V., 2001, ApJ, 557, 560
Petrosian V., 2003, in Bowyer S., Hwang C.-Y., eds, ASP Conf. Ser. Vol. 301, Matter and Energy in Clusters of Galaxies. Astron. Soc. Pac., San Francisco, p. 337
Petrosian V., Liu S., 2004, ApJ, 610, 550
Petrosian V., Yan H., Lazarian A., 2006, ApJ, 644, 603
Pfrommer C., Ensslin T. A., 2004, MNRAS, 352, 76
Pfrommer C., Springel V., Ensslin T. A., Jubelgas M., 2006, MNRAS, 367, 113
Pilipp W., Völk H. J., 1971, J. Plasma Phys., 6, 1
Ptuskin V. S., 1988, Sov. Astron. Lett., 14, 255
Reimer O., 2004, JKAS, 37, 307
Rephaeli Y., Gruber D., Arieli Y., 2006, ApJ, 649, 673
Ricker P. M., Sarazin C. L., 2001, ApJ, 561, 621
Roettiger K., Burns J. O., Loken C., 1996, ApJ, 473, 651
Roettiger K., Loken C., Burns J. O., 1997, ApJS, 109, 307

Ryu D., Kang H., Hallman E., Jones T. W., 2003, ApJ, 593, 599
Sarazin C. L., 1999, ApJ, 520, 529
Schekochihin A. A., Cowley S. C., 2006, Phys. Plasmas, 13, 56501
Schekochihin A. A., Cowley S. C., Kulsrud R. M., Hammett G. W., Sharma P., 2005, ApJ, 629, 139
Schlickeiser R., 2002, Cosmic Ray Astrophysics. Springer-Verlag, Berlin, Heidelberg
Schlickeiser R., Miller J. A., 1998, ApJ, 492, 352
Schlickeiser R., Sievers A., Thiemann H., 1987, A&A, 182, 21
Schuecker P., Finoguenov A., Miniati F., Boehringer H., Briel U. G., 2004, A&A, 426, 387
Shafranov V. D., 1967, Reviews of Plasma Physics, Vol., 3. Consultants Bureau, New York
Shebalin J. V., Montgomery D., 1988, J. Plasma Phys., 39, 339
Shebalin J. V., Matthaeus W. H., Montgomery D., 1983, J. Plasma Phys., 29, 525
Simon A., 1955, Phys. Rev., 100, 1557
Steinacker J., Miller J. A., 1992, ApJ, 393, 764
Subramanian K., Shukurov A., Haugen N. E. L., 2006, MNRAS, 366, 1437
Sun M., Jones C., Forman W., Nulsen P. E. J., Donahue M., Voit G. M., 2006, ApJ, 637, L81
Sunyaev R. A., Norman M. L., Bryan G. L., 2003, Astron. Lett. 29, 783
Takizawa M., Naito T., 2000, ApJ, 535, 586
Tsytovich V. N., 1972, An Introduction to the Theory of Plasma Turbulence. Pergamon Press, Oxford
Tsytovich V. N., 1977, Theory of Turbulent Plasma. Consultant Bureau, New York
Vazza F., Tormen G., Cassano R., Brunetti G., Dolag K., 2006, MNRAS, 369, L14
Vogt C., Ensslin T. A., 2005, A&A, 434, 67
Voigt L. M., Fabian A. C., 2004, MNRAS, 347, 1130
Völk H. J., Atoyan A. M., 1999, Astropart. Phys., 11, 73
Völk H. J., Aharonian F. A., Breitschwerdt D., 1996, Space Sci. Rev., 75, 279
Yan H., Lazarian A., 2002, Phys. Rev. Lett., 89, 1102
Yan H., Lazarian A., 2004, ApJ, 614, 757
Zank G. P., Matthaeus W. H., 1992, J. Geophys. Res., 97, 189
Zank G. P., Matthaeus W. H., 1993, Phys. Fluids A, 5, 257
Zhou Y., Matthaeus W. H., 1990, J. Geophys. Res., 95, 14881

APPENDIX A: DIELECTRIC TENSOR IN THE LONG WAVELENGTH LIMIT

A relevant case for many astrophysical situations is that of long-wavelength modes for which it is $|z_\alpha| \sim kp/m_\alpha\Omega_{\rm o}^\alpha \ll 1$. This is also the case of the turbulent modes in the ICM of interest in the present paper. The dielectric tensor (equation 16) is in the form

$$K_{ij} = \delta_{ij} - \omega^{-2} \sum_\alpha R_{ij}^\alpha \tag{A1}$$

BS73 calculated the tensor R_{ij} from equations (16)–(17) and under the conditions $z_\alpha = k_\perp p_\perp/m_\alpha\Omega_{\rm o}^\alpha \ll 1$ and $X_1^\alpha \equiv (k_\parallel p_\parallel/m_\alpha - \omega\gamma)/\Omega_{\rm o}^\alpha \ll 1$. In this case, by taking into account that $J_n(z_\alpha) = (z_\alpha/2)^n \sum_m (-z_\alpha^2/4)^m/m!\Gamma(n+m+1)$, one finds (BS73)

$$R_{ij} \simeq -2\pi \sum_\alpha \omega_{{\rm p},\alpha}^2 \int_{\rm o}^\infty {\rm d}p_\perp \int_{-\infty}^\infty {\rm d}p_\parallel \left\{ p_\perp^2 \Lambda_{ij}^\alpha \left[(\omega - k_\parallel v_\parallel) \frac{\partial \hat{f}_\alpha(p)}{\partial p_\perp} + k_\parallel v_\perp \frac{\partial \hat{f}_\alpha(p)}{\partial p_\parallel} \right] + m_\alpha p_\parallel \left(v_\perp \frac{\partial \hat{f}_\alpha(p)}{\partial p_\parallel} - v_\parallel \frac{\partial \hat{f}_\alpha(p)}{\partial p_\perp} \right) \delta_{i3}\delta_{j3} \right\}, \tag{A2}$$

where

$$\Lambda_{ij}^\alpha = \frac{1}{2\Omega_{\rm o}^\alpha} \begin{pmatrix} X_1^\alpha & -{\rm i} & -\left(\frac{p_\parallel}{p_\perp}\right) z_\alpha \\ {\rm i} & X_1^\alpha - \frac{z_\alpha^2}{2X_1^\alpha} & -{\rm i}\left(\frac{p_\parallel}{p_\perp}\right) \frac{z_\alpha}{X_1^\alpha} \\ -\left(\frac{p_\parallel}{p_\perp}\right) z_\alpha & {\rm i}\left(\frac{p_\parallel}{p_\perp}\right) \frac{z_\alpha}{X_1^\alpha} & \frac{z_\alpha^2 - 2}{X_1^\alpha} \left(\frac{p_\parallel}{p_\perp}\right)^2 \end{pmatrix} + \mathcal{O}\left(z_\alpha^2\right) \tag{A3}$$

and where the term $\mathcal{O}(z_\alpha^2)$ comes from the contribution from the $n \geqslant 2$ resonances in equation (16).

In an isotropic plasma, equations (A2)–(A3) can be further simplified by introducing the total energy of species α:

$$\mathcal{E}_\alpha = 2\pi N_\alpha \int\int {\rm d}p_\perp p_\perp {\rm d}p_\parallel \hat{f}_\alpha(p) m_\alpha c^2 \gamma, \tag{A4}$$

and the pressure of species α:

$$P_\alpha = P_\perp^\alpha = \pi N_\alpha \int\int {\rm d}p_\perp p_\perp {\rm d}p_\parallel \hat{f}_\alpha(p) p_\perp v_\perp = P_\parallel^\alpha = 2\pi N_\alpha \int\int {\rm d}p_\perp p_\perp {\rm d}p_\parallel \hat{f}_\alpha(p) p_\parallel v_\parallel \tag{A5}$$

which is $P_\alpha = N_\alpha k_{\rm B} T$ for a Maxwellian distribution of α particles.

By integrating equations (A2) and (A3), introducing equations (A4) and (A5), and requiring no net charge in the plasma (i.e. $\sum_\alpha N_\alpha e_\alpha = 0$), the components of the tensor are given by

$$R_{11} = -\frac{4\pi k_\parallel^2 c^2}{B_{\rm o}^2} \left(\frac{\omega}{k_\parallel c} \right)^2 \sum_\alpha \left(\mathcal{E}_\alpha + P_\alpha \right), \tag{A6}$$

$$R_{12} = R_{21} = 0, \tag{A7}$$

$$R_{13} = R_{31} = 0, \tag{A8}$$

$$R_{22} = R_{11} + \frac{8\pi k_\perp^2 c^2}{B_o^2}\sum_\alpha P_\alpha - \sum_\alpha \frac{\pi k_\perp^2 N_\alpha}{B_o^2}\left\langle p_\perp v_\perp^3\right\rangle_\alpha - \frac{2\pi^2 k_\parallel k_\perp^2 c^2}{B_o^2}\sum_\alpha N_\alpha \int\int p_\perp \mathrm{d}p_\perp \mathrm{d}p_\parallel \frac{p_\perp^2 v_\perp^2}{\omega - k_\parallel v_\parallel}\frac{\partial \hat{f}_\alpha(p)}{\partial p_\parallel}, \tag{A9}$$

$$R_{23} = -R_{32} = -\frac{4\pi^2 \mathrm{i} k_\perp c}{B_o}\sum_\alpha N_\alpha e_\alpha \omega \int\int p_\perp \mathrm{d}p_\perp \mathrm{d}p_\parallel \frac{p_\perp v_\perp}{\omega - k_\parallel v_\parallel}\frac{\partial \hat{f}_\alpha(p)}{\partial p_\parallel}, \tag{A10}$$

$$R_{33} = -\frac{8\pi^2\omega^2}{k_\parallel}\sum_\alpha N_\alpha e_\alpha^2 \int\int p_\perp \mathrm{d}p_\perp \mathrm{d}p_\parallel \frac{1}{\omega - k_\parallel v_\parallel}\frac{\partial \hat{f}_\alpha(p)}{\partial p_\parallel}, \tag{A11}$$

which give all the components of the dielectric tensor when inserted in equation (A1).

As usual, the integrals in equations (A9)–(A11) can be calculated using the *Sokhotskii–Plamelj* formula by taking into account the causal condition (e.g. Melrose 1968):

$$\frac{1}{\omega - k_\parallel v_\parallel + \mathrm{i}0} = \mathcal{P}\frac{1}{\omega - k_\parallel v_\parallel} - \mathrm{i}\pi\delta(\omega - k_\parallel v_\parallel), \tag{A12}$$

where $\mathcal{P}$ is the *Cauchy principal value*, and i0 is an infinitesimal imaginary term.

APPENDIX B: ENERGY OF THE MODE

The energy of the mode in a collisionless plasma is given by (e.g. Barnes 1968; Melrose 1968)

$$W(k,\omega) = \frac{1}{16\pi}\left[B_{ki}^* B_{ki} + E_{ki}^* \frac{\partial}{\partial\omega}\left(\omega K_{ij}^{\mathrm{h}}\right)E_{kj}\right]_{\omega_\mathrm{i}=0}, \tag{B1}$$

where K_{ij}^{h} stands for the Hermitian part of the dielectric tensor (A1). In the weak damping limit (i.e. $Im(\omega) \ll 1$) the Hermitian part of the dielectric tensor (equation A1) can be expressed as

$$K_{ij}^{\mathrm{h}} \simeq \delta_{ij} - \sum_\alpha \left[\mathcal{M}_{ij,\alpha}^{\mathrm{h}}(\omega_\mathrm{r}) + \mathrm{Im}(\omega)\frac{\partial \mathcal{M}_{ij,\alpha}^{\mathrm{h}}(\omega_\mathrm{r})}{\partial\omega}\right], \tag{B2}$$

where the components of the tensor

$\mathcal{M}_{ij,\alpha} = (R_{ij}^\alpha + R_{ji}^\alpha)/2\omega^2$ are given by equations (A6)–(A11). We note that the x-component of the electric field associated with the mode (and its spatial Fourier transform) is 0 (equation 13), and thus only the components K_{22}^{h}, K_{23}^{h}, K_{32}^{h} and K_{33}^{h} contribute to equation (B1). The Hermitian part of the relevant components of the tensor $\mathcal{M}_{ij}$ are obtained from equations (A9)–(A12) and equation (B2):

$$\mathcal{M}_{22,\alpha}^{\mathrm{h}} = -\frac{4\pi}{B_o^2}(\mathcal{E}_\alpha + P_\alpha) + \left(\frac{k_\perp c}{\omega_\mathrm{r}}\right)^2\left(\frac{8\pi P_\alpha}{B_o^2} - \frac{\pi N_\alpha\langle p_\perp v_\perp^3\rangle}{B_o^2 c^2}\right) - 2\pi^2\frac{k_\parallel k_\perp^2 N_\alpha c^2}{B_o^2\omega_\mathrm{r}^2}\int_0^\infty \mathrm{d}p_\perp p_\perp^3 v_\perp^2\left(\mathcal{P}\int\frac{\mathrm{d}p_\parallel}{\omega_\mathrm{r} - k_\parallel v_\parallel}\frac{\partial\hat{f}(p)}{\partial p_\parallel}\right)_\alpha, \tag{B3}$$

$$\mathcal{M}_{23,\alpha}^{\mathrm{h}} = -\mathcal{M}_{32,\alpha}^{\mathrm{h}} = -4\pi^2\frac{k_\perp N_\alpha c e_\alpha}{B_o\omega_\mathrm{r}}\mathrm{i}\int_0^\infty \mathrm{d}p_\perp p_\perp^2 v_\perp\left(\mathcal{P}\int\frac{\mathrm{d}p_\parallel}{\omega_\mathrm{r} - k_\parallel v_\parallel}\frac{\partial\hat{f}(p)}{\partial p_\parallel}\right)_\alpha, \tag{B4}$$

$$\mathcal{M}_{33,\alpha}^{\mathrm{h}} = -\frac{8\pi^2 N_\alpha e_\alpha^2}{k_\parallel}\int_0^\infty \mathrm{d}p_\perp p_\perp\left(\mathcal{P}\int\frac{\mathrm{d}p_\parallel}{\omega_\mathrm{r} - k_\parallel v_\parallel}\frac{\partial\hat{f}(p)}{\partial p_\parallel}\right)_\alpha. \tag{B5}$$

The energy spectrum of the mode (equation B1) is thus given by

$$W(k,\omega) = \frac{1}{16\pi}\left\{|B_k|^2 + |E_k|^2 - |E_\perp|^2\frac{\partial}{\partial\omega}\left(\omega\sum_\alpha\mathcal{M}_{22,\alpha}^{\mathrm{h}}\right) - |E_\parallel|^2\frac{\partial}{\partial\omega}\left(\omega\sum_\alpha\mathcal{M}_{33,\alpha}^{\mathrm{h}}\right) - \left[E_\perp^* E_\parallel - E_\perp E_\parallel^*\right]\frac{\partial}{\partial\omega}\left(\omega\sum_\alpha\mathcal{M}_{23,\alpha}^{\mathrm{h}}\right)\right\} \tag{B6}$$

Here, it is necessary to evaluate the ratio between the parallel and perpendicular fluctuations of the electric field in equation (B6). In the low amplitude regime the Fourier–Laplace transform of the mode electric field satisfies $\Psi\cdot\boldsymbol{E}(\boldsymbol{k},\omega) = 0$, where $\Psi_{ij} = R_{ij} + c^2 k_i k_j - (k^2c^2 - \omega^2)\delta_{ij}$ is the *Maxwell operator* (e.g. Melrose 1968; BS73; Schlickeiser 2002). Thus since it is $E_{k1} = 0$, one has

$$\frac{E_\parallel}{E_\perp} = -\frac{\Psi_{12} + \Psi_{22} + \Psi_{32}}{\Psi_{13} + \Psi_{23} + \Psi_{33}}. \tag{B7}$$

A dimensional analysis of *Maxwell operator* in case of the long-wavelength modes gets $\Psi_{32} \gg \Psi_{22} \gg \Psi_{12}$ and $\Psi_{33} \gg \Psi_{23} \gg \Psi_{13}$ (BS73), and thus the ratio between the perpendicular and parallel component of the mode electric field is

$$E_\perp \simeq -E_\parallel\frac{R_{33}}{R_{32}} \tag{B8}$$

which can be used in equation (B6) in combination with equations (A10) and (A11). Here, it should be noticed that it is $|E_\perp|^2/|E_\parallel|^2 \approx |R_{33}|^2/|R_{32}|^2 \gg 1$ and thus that the fluctuations of the electric field are perpendicular to B_o, and to the fluctuations of the magnetic field (see equations 12–14). On the other hand, this does not immediately imply that the contribution from $|E_\perp|^2$ in equation (B6) dominate on that from $|E_\parallel|^2$: a dimensional analysis of the elements of the tensor R_{ij} indeed shows that $|E_\perp|^2\mathcal{M}_{22}$ is of the same order of $|E_\parallel|^2\mathcal{M}_{33}$.

The most important contribution of particles to the spectrum of the mode in the ICM (as in many other astrophysical cases) is provided by thermal electrons and protons which dominates the energy budget of the plasma. In this case the particle distribution function of electrons and protons is Maxwellian:

$$f_\alpha(p) = N_\alpha \hat{f}_\alpha(p) = \frac{N_\alpha}{(2\pi)^{3/2}} \frac{\exp\left\{-p^2/(2m_\alpha k_\mathrm{B} T)\right\}}{(m_\alpha k_\mathrm{B} T)^{3/2}} \tag{B9}$$

and, from equations (B3)–(B5), the components of the Hermitian part of the dielectric tensor become

$$\mathcal{M}^\mathrm{h}_{22,\alpha} = -\frac{4\pi}{B_\mathrm{o}^2}(\mathcal{E}+P)_\alpha + \left(\frac{k_\perp c}{\omega_\mathrm{r}}\right)^2 \left(\frac{8\pi P_\alpha}{B_\mathrm{o}^2} - \frac{\pi N_\alpha \left\langle p_\perp v_\perp^3 \right\rangle}{B_\mathrm{o}^2 c^2}\right) + \frac{A^\alpha_{22}}{\omega^2}\mathcal{I}_\alpha M^\alpha_{22} + \frac{A^\alpha_{22}}{\omega_\mathrm{r}^2}\mathcal{I}_\alpha, \tag{B10}$$

$$\mathcal{M}^\mathrm{h}_{23,\alpha} = \frac{A^\alpha_{23}}{\omega}\mathrm{i}\mathcal{I}_\alpha, \tag{B11}$$

$$\mathcal{M}^\mathrm{h}_{33,\alpha} = A^\alpha_{33}\mathcal{I}_\alpha, \tag{B12}$$

where $\mathcal{I}_\alpha$ stands for the Cauchy principal value in equations (B3)–(B5), and we put

$$A^\alpha_{22} = \frac{16\pi^2}{(2\pi)^{3/2}} \frac{k_\parallel k_\perp^2 c^2 N_\alpha}{B_\mathrm{o}^2 m_\alpha^2} \sqrt{m_\alpha k_\mathrm{B} T}, \tag{B13}$$

$$A^\alpha_{23} = \frac{8\pi^2}{(2\pi)^{3/2}} \frac{N_\alpha e_\alpha k_\perp c}{B_\mathrm{o} m_\alpha^{3/2} k_\mathrm{B}^{1/2} T^{1/2}} \tag{B14}$$

and

$$A^\alpha_{33} = \frac{8\pi^2}{(2\pi)^{3/2}} \frac{N_\alpha e_\alpha^2}{(m_\alpha k_\mathrm{B} T)^{3/2} k_\parallel}. \tag{B15}$$

In the case of Maxwellian distributions the Cauchy principal value in equations (B10)–(B12) reads

$$\mathcal{I}_\alpha = \left[\mathcal{P}\int_{-\infty}^{\infty} \frac{\mathrm{d}p_\parallel p_\parallel}{\omega_\mathrm{r} - k_\parallel v_\parallel} \exp\left(-\frac{p_\parallel^2}{2m_\alpha k_\mathrm{B} T}\right)\right]_\alpha = -\sqrt{2\pi}(m_\alpha k_\mathrm{B} T)^{1/2} \frac{m_\alpha}{k_\parallel}[1 - \tilde{\omega}_\alpha F(\tilde{\omega}_\alpha)], \tag{B16}$$

where we define

$$F(\tilde{\omega}) \equiv 2\exp\left\{-\tilde{\omega}_\alpha^2\right\} \int_0^{\tilde{\omega}_\alpha} \mathrm{d}x \exp\{x^2\} \rightarrow \left\{ \begin{array}{ll} 2\tilde{\omega}_\alpha - \frac{4}{3}\tilde{\omega}_\alpha^3 + \frac{8}{15}\tilde{\omega}_\alpha^5 & \text{for } \tilde{\omega} \gg 1 \\ \\ \frac{1}{\tilde{\omega}_\alpha} + \frac{1}{2\tilde{\omega}_\alpha^3} + \frac{3}{4\tilde{\omega}_\alpha^5} & \text{for } \tilde{\omega} \ll 1 \end{array} \right\} \tag{B17}$$

which for real argument is $F(x) = -\mathcal{R}Z(x)$, and

$$Z(x) = \frac{1}{\sqrt{\pi}} \int_{-\infty}^{\infty} \frac{\mathrm{d}t \exp\{-t^2\}}{t - x} \tag{B18}$$

is the well-known *plasma dispersion function* (Fried & Conte 1961; Melrose 1968; Percival & Robinson 1998). The adimensional frequency, $\tilde{\omega}$, in equation (B17) is defined (from equation 4) as

$$\tilde{\omega}_\alpha(\beta_\mathrm{pl}, \theta) = \omega \frac{m_\alpha}{k_\parallel} \frac{1}{\sqrt{2m_\alpha K_\mathrm{B} T}} = \sqrt{\frac{5}{3}} \left(\frac{k}{k_\parallel}\right) \left(\frac{m_\alpha}{m_\mathrm{p}}\right)^{1/2} \left(\frac{\beta_\mathrm{pl}/2+1}{\beta_\mathrm{pl}}\right)^{1/2} \left\{1 + \sqrt{1 - 4\left(\frac{k}{k_\parallel}\right)^2 \frac{\beta_\mathrm{pl}/2}{(1+\beta_\mathrm{pl}/2)^2}}\right\}^{1/2}. \tag{B19}$$

For $\tilde{\omega}_\alpha \sim 1$ the bulk of thermal particles of species α undergoes $n = 0$ resonance with the mode. The value of $\tilde{\omega}_\alpha$ increases with increasing θ and goes to infinity with $\theta \rightarrow \pi/2$. For a given $(\theta, \beta_\mathrm{pl})$ the value of the adimensional frequency of electrons is about 40 times smaller than that of protons, thus electrons experience $n = 0$ resonance with the mode at larger angles than protons. The value of the adimensional frequency also depends on the β_pl: $\tilde{\omega}_\alpha$ increases with decreasing β_pl, while $\tilde{\omega}_\alpha \rightarrow \sqrt{5/3}\sqrt{m_\alpha/m_\mathrm{p}}/\cos(\theta)$ for large β_pl.

The behaviour of the Cauchy principal value (equation B16) and of $F(\tilde{\omega}_\alpha)$ is driven by the value of $\tilde{\omega}_\alpha$. In Fig. B1 we report $F(\tilde{\omega})$ for electrons and protons for different values of β_pl. F peaks at $\tilde{\omega} \sim 1$ and for electrons this happens at larger θ than for protons. With decreasing β_pl the phase velocity of the mode increases and becomes significantly larger than the sound speed. This causes a shift of the peak of F towards smaller θ in Fig. B1, and also prevents the $n = 0$ resonance of the bulk of the protons in the case of small β_pl. In Fig. B2 we report the Cauchy principal value (equation B16) of thermal electrons and protons. The principal value goes to zero for $\theta \rightarrow \pi/2$ which essentially means that in this limit there is no particle–mode coupling via the $n = 0$ resonance, and this is because formally infinite particle's velocity is requested to resonate at these angles. Also in this case the features of the curves are shifted at smaller angles with decreasing β_pl.

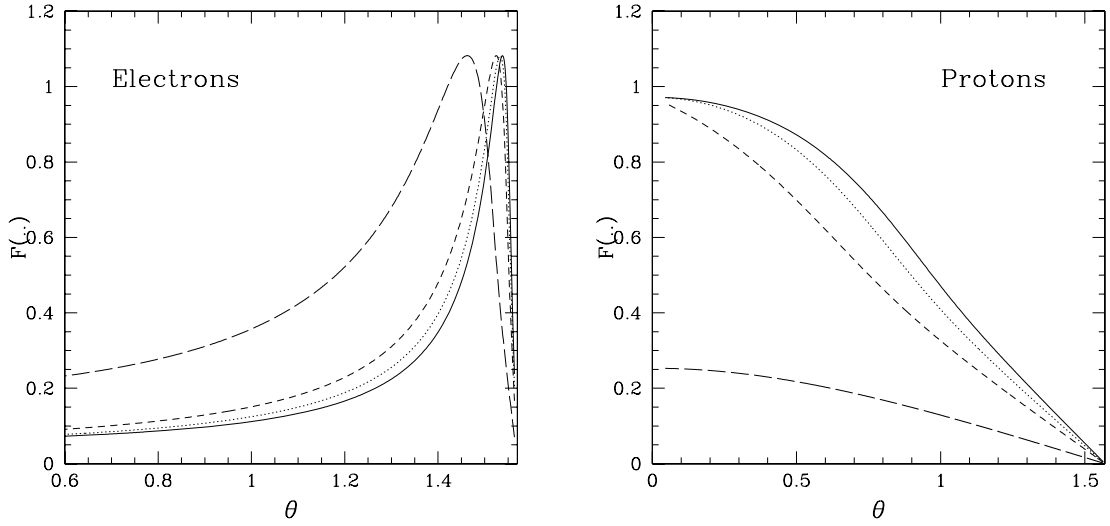

Figure B1. The function F is reported, as a function of the mode-propagation angle θ, for electrons (left-hand panel) and for protons (right-hand panel). Results are shown for different values of c_s^2/v_A^2 ($=\beta_{pl}/2$): 100 (solid lines), 3 (dotted lines), 1 (dashed lines), 0.1 (long–dashed lines). In the calculations $k_B T = 8.6$ keV is assumed.

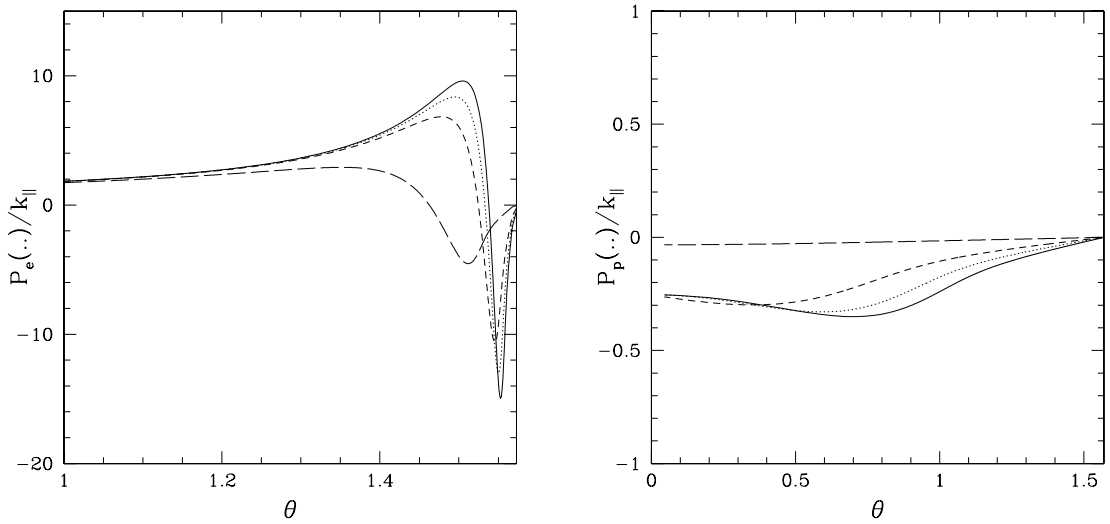

Figure B2. The function $\mathcal{P}(\cdots)/k_\parallel$ is reported, as a function of the mode-propagation angle θ, for electrons (left-hand panel) and protons (right-hand panel). Assumptions and line styles are the same as in Fig. B1.

Given these results, the spectrum of the mode (equation B6) in a magnetized-collisionless plasma can thus be obtained in explicit form. After some tedious algebra, from equation (B6), equations (B10)–(B17) and equation (B8) we find

$$W(k,\omega) = \frac{|B_k|^2}{16\pi}\left\{1 + \frac{(\omega/kc)^2}{1-\left(k_\parallel/k\right)^2 \frac{1}{1+\omega^2\left\langle A_{33}^2/A_{23}^2\right\rangle}}\left[1 + \frac{\omega^2\left\langle A_{33}^2/A_{23}^2\right\rangle}{1+\omega^2\left\langle A_{33}^2/A_{23}^2\right\rangle}\sum_\alpha\left\{\frac{N_\alpha m_\alpha c^2 + P_\alpha}{B_o^2/4\pi} + \frac{P_\alpha}{B_o^2/8\pi}\left(\frac{k_\perp c}{\omega}\right)^2\right.\right.\right.$$
$$\left.\left.\left.\times\left[1 - \mathcal{L}_\alpha\left(1 - \frac{\Delta_\alpha^{\mathcal{L}}}{2\mathcal{A}_2(\beta_{pl},\theta)}\right) - \frac{N_\alpha\left\langle p_\perp v_\perp^3\right\rangle_\alpha}{8P_\alpha c^2}\right]\right\}\right]\right\}, \tag{B20}$$

where we put

$$\mathcal{A}_2(\beta_{pl},\theta) = \frac{(1-\tilde{\omega}_p F_{\tilde{\omega}_p})^2\left(1+\frac{1-\tilde{\omega}_e F_{\tilde{\omega}_e}}{1-\tilde{\omega}_p F_{\tilde{\omega}_p}}\right)^2 + \frac{5\pi}{3}\frac{V_{ph}^2}{c_s^2}\left(\frac{k}{k_\parallel}\right)^2\exp\left(-2\tilde{\omega}_p^2\right)\left[1-\left(\frac{m_e}{m_p}\right)\exp\left(2\Delta\tilde{\omega}_{p-e}^2\right)\right]}{(1-\tilde{\omega}_p F_{\tilde{\omega}_p})^2\left[1-\frac{1-\tilde{\omega}_e F_{\tilde{\omega}_e}}{1-\tilde{\omega}_p F_{\tilde{\omega}_p}}\right]^2 + \frac{5\pi}{3}\frac{V_{ph}^2}{c_s^2}\left(\frac{k}{k_\parallel}\right)^2\exp(-2\tilde{\omega}_p^2)\left[1-\left(\frac{m_e}{m_p}\right)^{1/2}\exp\left(\Delta\tilde{\omega}_{p-e}^2\right)\right]^2}, \tag{B21}$$

where $\Delta\tilde{\omega}^2_{\rm p-e} = \tilde{\omega}^2_{\rm p} - \tilde{\omega}^2_{\rm e}$, and

$$\left\langle \frac{A^2_{33}}{A^2_{23}} \right\rangle = \frac{e^2_{\rm p} B^2_{\rm o}}{(k_\perp c)^2 (k_{\rm B} T)^2 k^2_\parallel} \mathcal{A}_2(\beta_{\rm pl}, \theta), \tag{B22}$$

and where

$$\Delta^{\mathcal{L}}_\alpha(\beta_{\rm pl}, \theta) = \frac{1 - \tilde{\omega}_\alpha F_{\tilde{\omega}_\alpha}(1 - a_\alpha) + 2 a_\alpha \tilde{\omega}^2_\alpha (1 - \tilde{\omega}_\alpha F_{\tilde{\omega}_\alpha})}{\mathcal{L}_\alpha(\beta_{\rm pl}, \theta)}, \tag{B23}$$

with a_α defined as

$$a_{\rm e} = -1 - 2\mathcal{A}_1 \tag{B24}$$

and

$$a_{\rm p} = -1 + 2\mathcal{A}_1 \tag{B25}$$

in the case of electrons and protons, respectively,

$$\mathcal{A}_1(\beta_{\rm pl}, \theta) = \frac{\left(1 - \tilde{\omega}_{\rm p} F_{\tilde{\omega}_{\rm p}}\right)^2 \left[1 - \left(\frac{1 - \tilde{\omega}_{\rm e} F_{\tilde{\omega}_{\rm e}}}{1 - \tilde{\omega}_{\rm p} F_{\tilde{\omega}_{\rm p}}}\right)^2\right] + \frac{5\pi}{3} \frac{V^2_{\rm ph}}{c^2_{\rm s}} \left(\frac{k}{k_\parallel}\right)^2 \exp\left(-2\tilde{\omega}^2_{\rm p}\right) \left[1 - \left(\frac{m_{\rm e}}{m_{\rm p}}\right) \exp\left(2\Delta\tilde{\omega}^2_{\rm p-e}\right)\right]}{\left(1 - \tilde{\omega}_{\rm p} F_{\tilde{\omega}_{\rm p}}\right)^2 \left[1 - \frac{1 - \tilde{\omega}_{\rm e} F_{\tilde{\omega}_{\rm e}}}{1 - \tilde{\omega}_{\rm p} F_{\tilde{\omega}_{\rm p}}}\right]^2 + \frac{5\pi}{3} \frac{V^2_{\rm ph}}{c^2_{\rm s}} \left(\frac{k}{k_\parallel}\right)^2 \exp\left(-2\tilde{\omega}^2_{\rm p}\right) \left[1 - \left(\frac{m_{\rm e}}{m_{\rm p}}\right)^{1/2} \exp\left(\Delta\tilde{\omega}^2_{\rm p-e}\right)\right]^2} \tag{B26}$$

and where

$$\mathcal{L}_\alpha(\beta_{\rm pl}, \theta) = 1 + 2\tilde{\omega}^2_\alpha [1 - \tilde{\omega}_\alpha F(\tilde{\omega}_\alpha)]. \tag{B27}$$

The terms $\mathcal{A}_1$, $\mathcal{A}_2$ and $\mathcal{L}_\alpha$ are reported in Fig. B3 for different values of $\beta_{\rm pl}$.

From equation (B20) with $(\omega^2 \langle A^2_{33}/A^2_{22} \rangle) \gg 1$, and $\omega = V_{\rm ph} k$, one gets the expression for the ratio between energy density in the magnetic field fluctuations and total energy density of the mode which is used in this paper:

$$\frac{|B_k|^2}{W(k, \theta)} \simeq 16\pi \left\{ 1 + \frac{\beta_{\rm pl}}{2} \left[\left(\frac{V_{\rm ph}}{c_{\rm s}}\right)^2 + \frac{3}{5} \left(\frac{k_\perp}{k}\right)^2 (2 - \mathcal{S}(\beta_{\rm pl}, \theta)) + \frac{1}{\beta_{\rm pl}} \left(\frac{V_{\rm ph}}{c}\right)^2 \left(\frac{3}{5}\beta_{\rm pl} + 2\right) \right] \right\}^{-1}, \tag{B28}$$

where

$$\mathcal{S}(\beta_{\rm pl}, \theta; \{f_{\rm rel}(p), T\}) = \sum_{\alpha = e, p} \mathcal{L}_\alpha(\beta_{\rm pl}, \theta) \left(1 - \frac{\Delta^{\mathcal{L}}_\alpha}{2\mathcal{A}_2(\beta_{\rm pl}, \theta)}\right) - \frac{N_\alpha \left\langle p_\perp v^3_\perp \right\rangle_\alpha}{8 P_\alpha c^2} \tag{B29}$$

is reported in Fig. B4 for different values of $\beta_{\rm pl}$; the expression for $|B_k|^2/W$ (equations B28 and B29) is important in our calculations since it allows to obtain the value of the TTD-damping rate and of the TTD-acceleration efficiency (Sections 4.3–5.1).

Both $\mathcal{L}$ and $\mathcal{S}$ goes to zero for $\theta \to \pi/2$ (Figs B3 and B4) which means that there is no contribution to the energy of the mode via $n = 0$ resonance. Also at small θ the contribution to the energy of the mode due to particle-mode coupling via $n = 0$ resonance goes to zero (Fig. B4), and this is because in case of parallel propagation of the mode the compressible part (parallel) of the magnetic field fluctuations which drives the $n = 0$ resonance goes to zero, $B_3 = c k_\perp E_\perp/\omega$ (equation 14). Finally, the same arguments used to comment Figs B1 and B2 can be used here to explain the evolution of the behaviour of $\mathcal{L}$ and $\mathcal{S}$ with $\beta_{\rm pl}$.

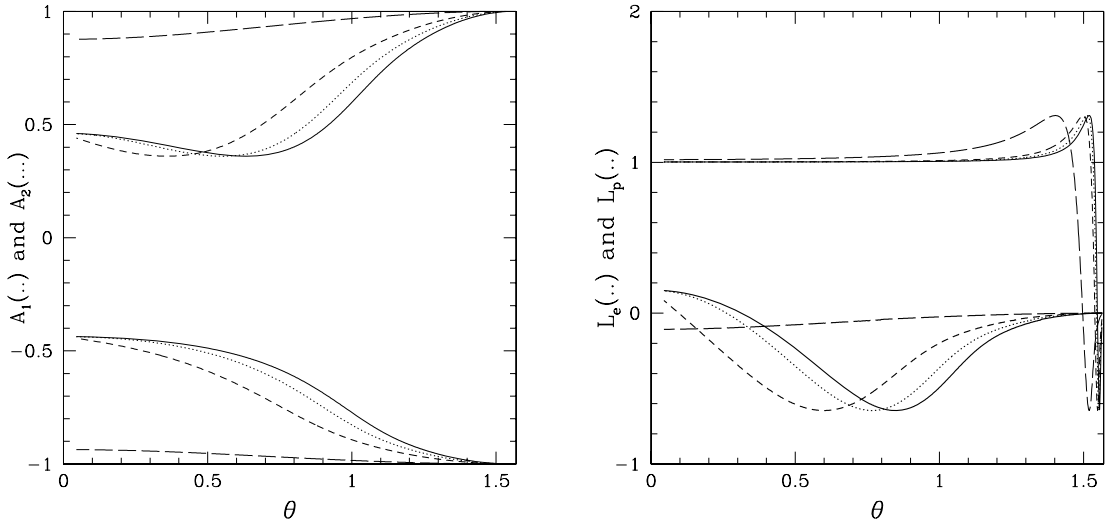

Figure B3. Left-hand panel: The expressions $\mathcal{A}_1$/ (bottom) and $\mathcal{A}_2$ (top) are reported as a function of the mode-propagation angle θ. Right-hand panel: The function $\mathcal{L}$ is reported, as a function of the mode-propagation angle θ, for electrons (thin lines) and for protons (thick lines). In both panels, assumptions and line styles are the same as in Fig. B1.

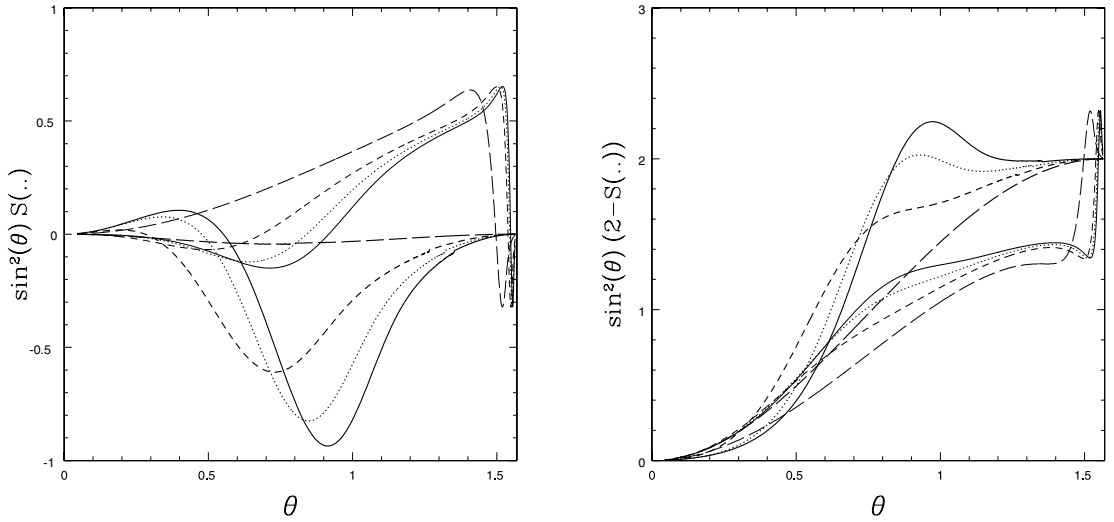

Figure B4. Left-hand panel: The expression $k_\perp^2 \mathcal{S}(\cdots)$ is reported as a function of the mode-propagation angle θ, for electrons (thin lines) and for protons (thick lines). Right-hand panel: The expression $k_\perp^2(2-\mathcal{S})$ is reported as a function of the mode-propagation angle θ, for electrons (thin lines) and for protons (thick lines). In both panels, assumptions and line styles are the same as in Fig. B1.

APPENDIX C: DAMPING COEFFICIENTS

The damping coefficient of the modes can be obtained by the standard formula for the linear growth rate of the modes in the weak damping approximation (e.g. Melrose 1968; BS73):

$$\Gamma = -\mathrm{i}\left(\frac{E_i^* K_{ij}^a E_j}{16\pi W}\right)_{\omega_\mathrm{i}=0} \omega_\mathrm{r}, \tag{C1}$$

where K_{ij}^a stands for the anti-Hermitian part of the dielectric tensor which can be directly obtained from equations (16) and (17); here we closely follow the approach in BS73. From the *Sokhotskii–Plamelj* formula (equation A12), from equation (17) one has (e.g. BS73):

$$E_i^*\left(\frac{V_i V_j^*}{\omega - n\Omega - k_\parallel v_\parallel}\right)_\alpha^a E_j \;\rightarrow\; -\mathrm{i}\pi\frac{\gamma}{k_\parallel}\delta\left(\omega_\mathrm{r}\frac{\gamma}{k_\parallel} - n\Omega_{o,\alpha}k_\parallel^{-1} - \frac{p_\parallel}{m_\alpha}\right)\left[v_\parallel^2 J_n(z_\alpha)^2|E_\parallel|^2 + \mathrm{i}v_\perp v_\parallel J_n(z_\alpha)J_n'(z_\alpha)\left(E_\perp E_\parallel^* - E_\perp^* E_\parallel\right)\right.$$
$$\left. + v_\perp^2 (J_n'(z_\alpha))^2|E_\perp|^2\right] = -\mathrm{i}\pi v_\perp^2\frac{\gamma}{k_\parallel}\delta\left(\omega_\mathrm{r}\frac{\gamma}{k_\parallel} - n\Omega_{o,\alpha}k_\parallel^{-1} - \frac{p_\parallel}{m_\alpha}\right)\left|\mathrm{i}J_n'(z_\alpha)E_\perp + \frac{p_\parallel}{p_\perp}J_n(z_\alpha)E_\parallel\right|^2. \tag{C2}$$

By making use of the properties of the δ functions, from equations (C1), (16) and (C2) one has

$$\Gamma = -\frac{\pi}{16\omega_\mathrm{r} W}\frac{k_\parallel}{|k_\parallel|}\sum_{\alpha,n}\omega_{\mathrm{p},\alpha}^2\int_0^\infty \mathrm{d}p_\perp\int_{-\infty}^\infty \mathrm{d}p_\parallel p_\perp^2\Psi_n^\alpha\left[\left(\frac{\omega}{k_\parallel} - v_\parallel\right)\frac{\partial\hat{f}_\alpha(p)}{\partial p_\perp} + v_\perp\frac{\partial\hat{f}_\alpha(p)}{\partial p_\parallel}\right]\;\delta\left(\frac{p_\parallel}{m_\alpha} + \frac{n\Omega_{o,\alpha} - \omega_\mathrm{r}\gamma}{k_\parallel}\right), \tag{C3}$$

where we define

$$\Psi_n^\alpha = 2\left|\mathrm{i}J_n'(z_\alpha)E_\perp + \frac{p_\parallel}{p_\perp}J_n(z_\alpha)E_\parallel\right|^2. \tag{C4}$$

Here we focus on the TTD case, $n = 0$, which is the most important resonance of long wavelength ($z_\alpha \ll 1$) fast modes and magnetosonic waves. In this case it is

$$\Psi_\mathrm{o}^\alpha \xrightarrow{z_\alpha \ll 1} 2\left|\frac{p_\parallel}{p_\perp}E_\parallel - \mathrm{i}\frac{k_\perp v_\perp \gamma}{2\Omega_\mathrm{o}}E_\perp\right|^2 \tag{C5}$$

and by using the properties of the δ functions in equation (C3) we obtained a general formula for the damping rate (TTD) with particles of α-species:

$$\Gamma_\alpha(k) = -\frac{\pi}{32}\frac{|E_\perp|^2}{W}\frac{k_\parallel k_\perp^2}{|k_\parallel|}\frac{\omega_{\mathrm{p},\alpha}^2}{\omega}\mathcal{H}\left(1 - \left|\frac{\omega}{k_\parallel c}\right|\right)\frac{\sqrt{1-[\omega/(k_\parallel c)]^2}}{m_\alpha^2\Omega_{o,\alpha}^2}\int_0^\infty \frac{\mathrm{d}p_\perp\, p_\perp^3}{\sqrt{1+\left(\frac{p_\perp}{m_\alpha c}\right)^2}}\left|\frac{p_\perp}{\sqrt{1-[\omega/(k_\parallel c)]^2}} + m_\alpha c\sigma_\alpha\right|^2\left[\frac{\partial\hat{f}_\alpha(p)}{\partial p_\parallel}\right]_{p_\parallel(\mathrm{res})}, \tag{C6}$$

where $\mathcal{H}(x)$ is the Heaviside step function (1 for $x > 0$, and 0 otherwise), the derivative of the particle distribution function should be evaluated at

$$p_\parallel(\mathrm{res}) = m_\alpha c\left(\frac{\omega_\mathrm{r}}{k_\parallel c}\right)\left[\frac{1+\left(\frac{p_\perp}{m_\alpha c}\right)^2}{1-\left(\frac{\omega}{k_\parallel c}\right)^2}\right]^{1/2} \tag{C7}$$

and σ_α is given by

$$\sigma_\alpha = 2\mathrm{i}\left(\frac{\omega}{k_\parallel c}\right)\left(\frac{\Omega_\mathrm{o}}{k_\perp c}\right)_\alpha \frac{E_\parallel/E_\perp}{1-[\omega/(k_\parallel c)]^2}\sqrt{1-\left(\frac{m_\alpha c}{p_\perp}\right)^2}. \tag{C8}$$

Since the fluctuations of the electric field are essentially perpendicular to B_o (Appendix B), it is $E_\parallel \to 0$ and $\sigma_\alpha \to 0$ and thus from the Faraday law (equation 14) the expression for the damping rate gets simplified:

$$\Gamma_\alpha(k) = -\frac{\pi^2}{8}\frac{|B_k|^2}{B_\mathrm{o}^2}\frac{\omega}{W}\left(\frac{k_\perp}{k}\right)^2\frac{k_\parallel}{|k_\parallel|}\frac{\mathcal{H}\left(1-\left|\frac{\omega}{k_\parallel c}\right|\right)N_\alpha/m_\alpha}{\sqrt{1-[\omega/(k_\parallel c)]^2}}\int_0^\infty \mathrm{d}p_\perp \frac{p_\perp^5}{\sqrt{1+\left(\frac{p_\perp}{m_\alpha c}\right)^2}}\left(\frac{\partial \hat{f}_\alpha(p)}{\partial p_\parallel}\right)_{p_\parallel(\mathrm{res})}. \tag{C9}$$

Thus from equation (C9) one obtains formulae appropriate for the case of the ICM:

$$\Gamma_{\mathrm{e/p}}(k,\theta) = \sqrt{\frac{\pi}{8}}\frac{|B_k|^2}{W(k,\theta)}\mathcal{H}\left(1-\frac{V_\mathrm{ph}}{c}\frac{k}{|k_\parallel|}\right)\frac{V_\mathrm{ph}^2}{B_\mathrm{o}^2}\left(\frac{k}{|k_\parallel|}\right)\left(\frac{k_\perp}{k}\right)^2\frac{(m_{\mathrm{e/p}}k_\mathrm{B}T)^{1/2}}{1-\left(\frac{V_\mathrm{ph}k}{ck_\parallel}\right)^2}N_{\mathrm{e/p}}\exp\left[-\frac{m_{\mathrm{e/p}}V_\mathrm{ph}^2}{2k_\mathrm{B}T}\frac{(k/k_\parallel)^2}{1-\left(\frac{V_\mathrm{ph}k}{ck_\parallel}\right)^2}\right]k \tag{C10}$$

in the case of thermal particles, and

$$\Gamma_{\mathrm{e/p}}(k,\theta) = -\frac{\pi^2}{8}\frac{|B_k|^2}{W(k,\theta)}\left(\frac{k_\perp}{k}\right)^2\left(\frac{k}{|k_\parallel|}\right)\mathcal{H}\left(1-\frac{V_\mathrm{ph}}{c}\frac{k}{|k_\parallel|}\right)\frac{N_{e^\pm/p}\ V_\mathrm{ph}^2}{B_\mathrm{o}^2}\ k\left[1-\left(\frac{V_\mathrm{ph}k}{ck_\parallel}\right)^2\right]^2\int_0^\infty p^4\,\mathrm{d}p\left[\frac{\partial \hat{f}_\alpha(p)}{\partial p}\right]_{\mathrm{e/p}} \tag{C11}$$

in the case of relativistic particles (see also BS73), where in obtaining equation (C11) from equation (C9), one takes

$$p_\parallel(\mathrm{res}) \to \left(\frac{\omega}{k_\parallel c}\right)\frac{p_\perp}{\sqrt{1-[\omega/(k_\parallel c)]^2}} \tag{C12}$$

which implies $p_\perp = p\sqrt{1-[\omega/(k_\parallel c)]^2}$, and the derivative of the distribution function is taken:

$$\left[\frac{\partial \hat{f}_\alpha(p)}{\partial p_\parallel}\right]_{p_\parallel(\mathrm{res})} = \left[\frac{\partial \hat{f}_\alpha(p)}{\partial p}\frac{p_\parallel}{p}\right]_{p_\parallel(\mathrm{res})} = \left(\frac{\omega}{k_\parallel c}\right)\frac{\partial \hat{f}_\alpha(p)}{\partial p}. \tag{C13}$$

This paper has been typeset from a TEX/LATEX file prepared by the author.